**The Thesis Committee for Ian Rostagno**
**Certifies that this is the approved version of the following Thesis:**

# Friction Reduction Optimization for Extended Reach and Horizontal Wells

**APPROVED BY**
**SUPERVISING COMMITTEE:**

Eric van Oort, Supervisor

Pradeepkumar Ashok

# Friction Reduction Optimization for Extended Reach and Horizontal Wells

**by**

**Ian Rostagno**

**Thesis**

Presented to the Faculty of the Graduate School of

The University of Texas at Austin

in Partial Fulfillment

of the Requirements

for the Degree of

**Master of Science in Engineering**

**The University of Texas at Austin**

**May 2019**

## Acknowledgements

First, I would like to thank my advisor, Dr. Eric van Oort, who not only was there to give me invaluable guidance during my project, but who also increased my passion for every aspect related to Drilling Engineering, and Dr. Pradeep Ashok for always being there to give me support and feedback any day of the week, at any time. Thanks to the rest of the members of the Rig Automation Drilling and Performance Improvement in Drilling (RAPID) team for sharing your thoughts in every group meeting we have had.

I would like to thank The University of Texas at Austin, the Fulbright Association, the Ministry of Education from Argentina, the Institute of International Education (IIE) and the Argentinian Institute of Petroleum and Gas in Houston (IAPGH) for trusting me with funding without which it would have been impossible to do my Master's. Thank you to every member of these organizations that made this possible. Special thanks to Guillermo Hitters from the IAPGH for your constant help in connecting me with important players from Oil and Gas companies in Argentina.

Many thanks to my beloved family, my dad Carlos and my mother Silvina, who were there 24/7 to give me their support, no matter what. Thank you to my sister Mayra, which helped me get here with the experience she has from doing her PhD in Florida. Thank you to my grandmother Poly, who every single time I went through a stressful or difficult situation lighted a candle to give me her strength from Argentina.

Finally, thanks to my family away from home, my friends Esteban, Gabo, Ruso, Tano, Emma, Richard, Lean, Pao, Lu and Betty for innumerable lunches, dinners and meetings in which we wouldn't stop laughing. You made living in a foreign country something natural, without you this experience would have been completely different. Thank you to all my other friends I made along the way, specially to all the "Fulbrighters"

I met with their incredibly minds and projects that motivated me to do the best I could in everything.

# Abstract

## Friction Reduction Optimization for Extended Reach and Horizontal Wells

Ian Rostagno, MSE

The University of Texas at Austin, 2019

Supervisor: Eric van Oort

With conventional oil and gas reservoirs declining, energy companies are constructing more complex wells to economically produce natural resources that were not accessible previously. Extended reach Offshore wells and horizontal unconventional land wells are just two examples of technologies developed to unlock challenging reserves. However, torque and drag in extended reach and horizontal wells with departures of ten thousand feet or more still constitute one of the main challenges and technical limitations for drilling. Offshore wells can experience high friction even with the use of rotary steerable systems. Additionally, directional land wells drilled with downhole steerable motor experience high friction because only the bit rotates while the rest of the string slides against the wellbore wall. This friction can produce complications such as low sliding and rotating rates of penetration, high tortuosity, poor hole cleaning, vibrations, premature downhole tools failure or bit damaging and connection back-offs. Additionally, it can stop the string from moving backwards or forwards and rotating, potentially ending up with an irreversibly stuck drillstring and a shorter-than-planned well.

In this work, we try to understand the influence of different agents on friction behavior and mitigation in deviated and horizontal wells, and how these agents can be used most effectively while drilling to improve drilling performance and wellbore quality.

# Table of Contents

# List of Tables

# List of Figures

# Chapter 1: Introduction

The motivation for drilling faster, safer and higher-quality wells continues while the industry develops hydrocarbon resources ranging from unconventional shale to deep offshore plays. The average cost for drilling and completing a horizontal well was reduced from eight to seven figures in just a few years by continuously improving procedures, tools and general knowledge on shale hydrocarbon exploitation (EIA, 2016). This success is projecting a growth in worldwide shale gas production from 12% in 2015, to 30% in 2040 from unconventional natural gas resources, with current developments mainly in the United States, Canada, China and Argentina (EIA, 2015).

The key to developing these hydrocarbon assets is the ability to drill extended reach and horizontal wells that are hydraulically fracked subsequently. In order to maximize the revenue of each well, lateral sections of more than ten thousand feet are drilled, with often more than forty fracturing stages. However, drilling a well with such geometry and complexity is not an easy task, especially when the reservoir is quite deep.

One of the main challenges for drilling deep directional wells is to overcome the friction between the drillstring and the wellbore wall. A continuous string of drill pipes and downhole tools apply torque and weight through a bit against the formation to remove rock. This string, which can be more than twenty thousand feet long, needs to be able to move forward, backwards and rotate in a well, which can have a ten thousand feet vertical section, a ninety-degree turn, and a ten thousand feet lateral section (Figure 1). Friction sets a technical limit on how far the string can get to without restricting its own movement or damaging any downhole tools or surface equipment.

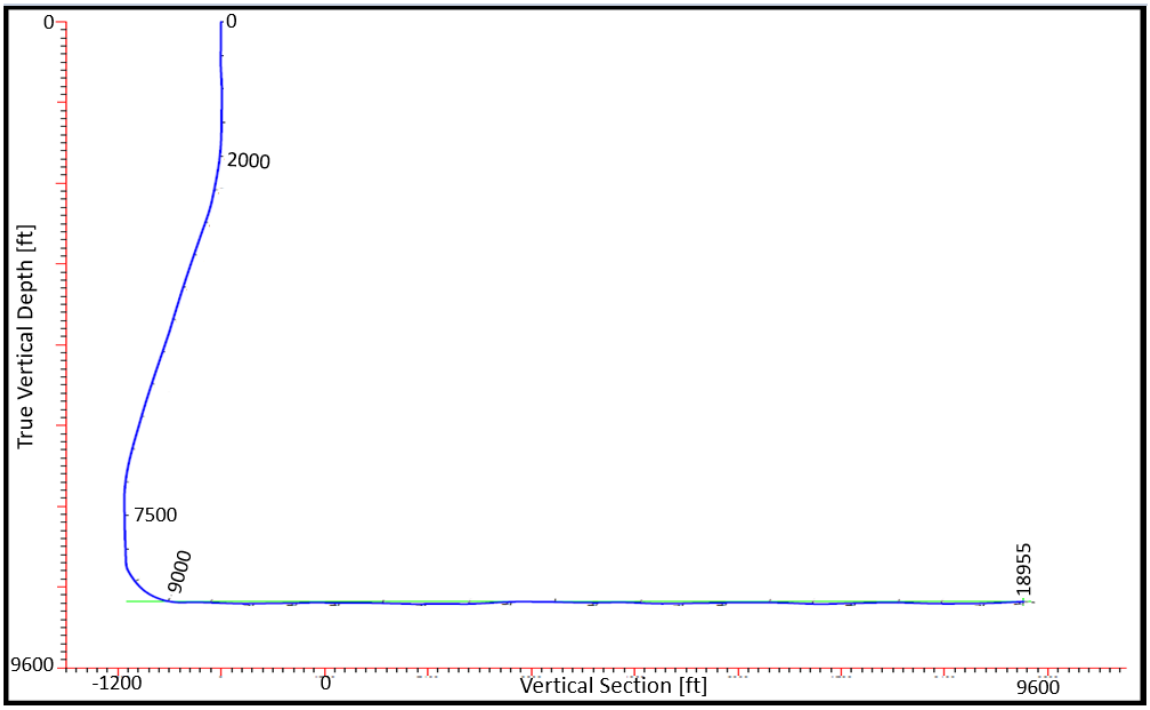


Figure 1: Lateral projection of a horizontal well. The blue line shows the final path of the well drilled.

When drilling directionally with a downhole motor, the drill pipe slides against the wellbore and encounters friction. This friction impairs force transfer to the bit, which reduces the rate of penetration (ROP) and also makes it difficult to achieve a desired drilling direction. The challenge in maintaining toolface direction increases deeper in the lateral sections of the well. As orienting the bit is a time-consuming process, an increase in the orientation process time ultimately increases the time it takes to finish drilling the well. Additionally, poor toolface control can translate into an increase in wellbore tortuosity, which in turn results in less efficient wellbore cleaning, increase in drag and a potential decrease in production rates in the future. Finally, poor hole cleaning and tortuosity may create restrictions whereby elastic energy gets stored in several sections of the drillstring,

producing poor weight transfer and a risk of releasing bursts of energy against the formation. This can potentially damage the bit and/or stalling the motor.

Several agents affect the friction forces during the operation, several of which can be controlled up to a certain point. This means that torque and drag needs to be considered from the early stages of well construction planning. Bottom Hole Assembly (BHA) and drillstring design, mud selection, the directional plan, and downhole tools selection can be altered, and surface operations can be deliberately manipulated to reduce friction. The type of formation will play an important role as well, but there is little to no control over this. The different factors affecting torque and drag will be described and analyzed here, with special focus on surface operations that can be done to mitigate friction to drill faster and farther. However, all these need to be used with caution, as additional and unintended drilling problems may happen. One example of this, covered later on in this thesis, is the risk of backing-off a connection during pipe rocking operations.

### 1.1 PRIOR WORK

Reduction in torque and drag allows for better force transfer to the bit, improving drilling performance and wellbore quality. For many years, several improvements were made to maximize friction mitigation, but further improvement opportunity still exists.

Drilling fluids have been a main topic of friction mitigation study. Oil-based muds (OBM) and synthetic oil-based muds (SOBM) have proven to reduce drag during tripping out and tripping in operations in relation to conventional water-based muds (WBM) (Kercheville et al., 1986). However, many additives were designed over the years, with evidence of WBMs outperforming OBMs (Yadav et al., 2015).

The type of drill pipes, heavy weight drill pipes, drill collars, stabilizers and other tools chosen for a drilling job also have an influence on friction. Higher clearance has been

found to be beneficial not only for reducing torque and drag, but also for improving hole cleaning (Rasi, 1994). Cuttings-beds accumulations are a problem for high deviation and horizontal wells, and so specific hole cleaning programs are usually required during the drilling operation (Guild et al., 1995).

Other major sources of friction are planned tortuosity, large scale-tortuosity and micro-scale tortuosity (Mason et al., 2005). Different directional plans can be considered to minimize planned tortuosity, but there is less control over the other two. Rotary Steerable Systems (RSS) have proven to reduce large scale-tortuosity, but they still produce spiraling around the wellbore axis that increases drag (Wijermans et al., 2001). Efforts to minimize friction involve decreasing all three types of tortuosities.

In addition, specific downhole tools have been developed to overcome static friction (Burnett et al, 2013). Drilling Agitator tools produce an oscillatory axial vibration that allows for kinetic friction instead of the much higher static friction (Rasheed, 2001). Finally, pipe rocking came about as a no-additional-cost technique for breaking friction in the shallower sections of a well, by rotating the drillstring on surface forward and backwards continuously, taking special care to maintain constant toolface (Duplantis, 2016).

### 1.2 Objectives, Contributions and Outline

The goal of this work is to provide the tools and knowledge required to maximize friction mitigation from the well planning to the operation stages to optimize drilling operations.

This thesis reviews the effect of the various agents involved in a drilling operation that affect torque and drag, and suggests design improvements that can be made during the early stages of well construction planning to diminish friction. Additionally, the efficiency

of downhole tools such as agitators is studied, and recommendations for placement in the drillstring are given according to available models. Finally, pipe rocking is studied thoroughly by reviewing how this technique is used in the industry currently, what can be done to improve its efficiency, what are the operational risks of using such a technique and what actions can be taken to reduce these risks.

First, background information on slide drilling techniques and torque and drag concepts are introduced in **Chapter 2**. Additionally, a comprehensive literature review summarizes state-of-the-art techniques for friction reduction in long-reach and horizontal wells. In this chapter, the influence of BHA and drillstring design, mud selection, directional plan, tortuosity, downhole friction reducers and pipe rocking in reducing friction is reviewed and current best practices for friction mitigation are presented.

A drillstring dynamics model is introduced in **Chapter 3**, with the final goal of simulating pipe rocking. The motivation for developing this simulator is to analyze rocking operations from real data and to anticipate what the optimum pipe rocking regime should be at each depth for various combinations of varying directional plans, BHAs, muds, etc.

Outputs of the pipe rocking model are validated against real field data in **Chapter 4**. Several simulations are performed to study the effect of different variables that can be controlled from surface during rocking operations. The final goal of these simulations is to establish the optimum rocking regime for a slide drilling operation. Additionally, an example of a drillstring back-off incident is shown and analyzed to explain why it may have happened and what could be done to reduce the risk of such incidents happening in the future.

This thesis ends with a summary of the work presented and highlights the major contributions (**Chapter 5**). Finally, recommendations and future work on this topic are suggested.

# Chapter 2: Background Information and Literature Review

Friction mitigation has been studied for many years. This chapter gives a general background on the physics behind dynamic and sliding friction management during directional drilling operations, and what is done in the field to mitigate friction. Additionally, current state-of-the-art technologies and practices for friction mitigation are presented.

## 2.1 Rotary vs Slide Drilling

A well is typically drilled by applying torque and weight from surface to the bit. With this action, cutters at the bit transfer weight and torque to the formation, forcing it to fail, thereby creating small cuttings which are brought back to surface by drilling mud (Mitchell et al., 2011). This operation is called rotary drilling because the whole string rotates. In rotary drilling mode, the well is expected to maintain an almost constant direction. To deviate the well, a directional assembly is needed.

For slide drilling operations, the BHA has a downhole steerable mud motor just above the bit, as shown in Figure 2. The mud motor has two main sections: the power section and the adjustable bent housing (Aguilera et al., 1991). The first one consists of a rotor and stator that generate torque and rotation when mud is pumped through it. Torque is then transmitted to the bit through a bearing section. Then, the adjustable bent housing section makes the bit have a small tilt in relation to the rest of the string, usually of less than two degrees. For directionally drilling the well, the whole string is kept stationary while mud is pumped so only the bit rotates. By doing this, the well follows the direction of the directed bit, creating a curve. For a successful sliding operation, the direction to which the bit is tilted must be kept constant. When this happens, the rest of the string slides against the wellbore wall (Maidla et al., 2004).

By this means, while the whole string is under dynamic friction in rotary mode, in slide drilling operations the string has to continuously break static friction to move forward. In horizontal wells, this friction can be a technical limitation to how far in the lateral the string can reach.

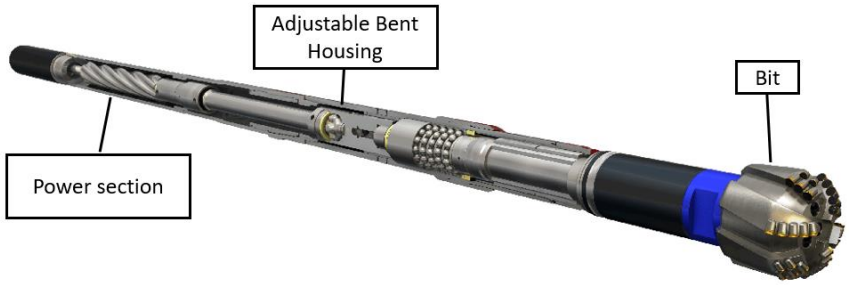


Figure 2: Scheme of a steerable downhole mud motor (Modified from Malcore, 2012).

Another way to directionally drill a well is by using a rotary steerable system (RSS) (Buker, 2001). The main difference between this and the conventional downhole motor is that with the RSS, the well path deviation is achieved with full rotation of the drillstring. One of the immediate consequences of this is that friction is much lower when deviating a well using a RSS assembly.

There are a variety of RSS systems on the market, but they all work in two different ways (Schaaf et al., 2000). Some of these tools are equipped with a non-rotating sleeve with pads that apply force against the formation, perpendicular to the well direction. A pivot stabilizer creates a temporary fulcrum, deviating the bit from the natural direction of the string. Other assemblies have the capability of deviating the direction of the bit from inside the tool, without pushing the formation and with fully rotating components. The first type is called Push-the-bit, while the second one is referred to as Point-the-bit. Bi-

directional communication between the surface and the tool lets the directional driller (DD) guide the tool to the desired inclination, azimuth and dog leg severity (DLS), and the RSS adapts to these instructions.

Rotary steerable systems can create more severe dog leg angles, drill faster and can drill longer intervals without failures (Sugiura et al., 2010). Drag is reduced and therefore higher ROP is typically achieved. Apart from that, the nature of the system creates much smoother and more precise well trajectories than when using a downhole motor. Finally, due to constant rotation of the drillstring, hole cleaning is improved, as cuttings are swept effectively from lower side of a high-angle or horizontal hole because of the rotary motion (Tomren et al., 1983).

The main disadvantage of RSS systems is their cost, as they can be significantly more expensive than a regular downhole motor. This is why their use is mainly restricted to offshore operations, while most land horizontal wells are still drilled with downhole motors (Warren, 2006).

Both the downhole motors and the rotary steerable systems work with a measurement while drilling (MWD) unit, which sends the position and other valuable information from downhole to the surface (Tanguy et al., 1981). MWD systems use accelerometers, magnetometers and gyroscopes to determine the tool inclination and azimuth during drilling. This information is then transmitted to surface through mud pulses and interpreted by the directional driller to estimate the position of the bit.

One of the challenges associated with this tool is that it is usually placed about forty to sixty feet away from the bit, so the DD has to extrapolate the data he or she gets to estimate the direction of the well. With ROPs that can be as low as 10 ft/hr, it can take six hours and more to reach the real position of the bit measured by the MWD.

Apart from that, surveys to determine the position and orientation of the tool are usually taken every ninety feet. As this is not a continuous measurement, the path in which the well varied from one survey to the other can be different and an approximation to determine the path must be made (Codling, 2017). For the rest of this thesis, the path approximation is done with the minimum curvature method (MCM), an accepted industry standard in which two successive points are assumed to lie on a circular arc located in a plane. For further information about this method, the reader can refer to Mitchell et al. (2011).

### 2.3 Problems During Slide Drilling Operations

As mentioned in the previous section, downhole steerable motors are currently the preferred candidate for directionally drilling of horizontal land wells due to their lower cost in relation to RSS systems. However, there are some potential drilling inefficiencies associated with the use of such tools.

The first downside of using them is that ROP is reduced compared to using a RSS. The reason for this is that the drag along the lateral section decreases the efficiency of weight transfer to the bit (Maidla et al., 2004). Due to this friction, surface measurements of weight onbBit (WOB) are unreliable and directional drillers generally use differential pressure (DP) to estimate how much force is actually applied against the formation.

Apart from that, it also takes additional time to orientate the tool in the desired direction, thereby decreasing gross ROP. Before a sliding operation, the DD sets an inclination and azimuth to which the well needs to be deviated. To do this, the string is pulled up and reciprocated to release any torque still held in it, and only then is the bit oriented. Through careful control of hook load, WOB, torque and DP, the DD tries to manage the wellbore trajectory constant with small surface adjustments. However, reactive

torque at the bit and sudden energy releases in the drillstring can deflect the string from the desired position necessitating its reorientation, a time-consuming process. As the well extends farther in the lateral section, the magnitude of drag increases and the difficulty to maintain toolface control becomes higher.

There are some other immediate consequences. Slide segments are not continuous, and the various changes between sliding and rotary drilling intervals result in a well trajectory that is not a smooth curve, but an amalgamation of straight segments and turns (Weijermans et al., 2001). Additionally, as corrections are continuously made to the trajectory, it is highly unlikely to follow the original plan precisely. Instead, the wellbore usually 'zig-zags' around the original plan, increasing the tortuosity of the well which will increase torque and drag.

Weight can suddenly be released from the bit against the formation, which apart from damaging the bit can also stall the downhole motor (Worford et al., 1983). When the bit cannot rotate while the pumps are still on, the drilling mud forces its way through the power section, eroding the stator and potentially failing the motor. Such failure is one of the main reasons why BHAs are often pulled out prematurely when drilling a long lateral section (Alley et al., 1991). Depending on how deep the BHA is, this process can take several hours or even days.

Finally, cuttings accumulate in the low side of the horizontal lateral section because the string is not rotating during slides. Pipe rotation facilitates rotary motion of the cuttings and turbulent flow, increasing the fluid's capability to transport cuttings (Tomren et al., 1983). With a stationary string, a cuttings bed accumulates, which can create a hole cleaning problem that in turn increases drag. If not properly addressed, this can lead to a stuck string in the wellbore.

## 2.4 STATE-OF-THE-ART PRACTICES FOR FRICTION MITIGATION

In this section, we will investigate the different factor / agents that influence torque and drag in deviated wells.

Sliding friction force is often calculated by multiplication of the normal force with a friction factor. Therefore, efforts for reduction in torque and drag are focused either on reducing the contact force or decreasing the friction coefficient. This friction factor can be estimated by calibration from experimental data, and some typical values for different base muds have been reported in the works of Alfsen et al. (1993), Guild et al. (1993), Mueller et al. (1991) and Kimball III et al. (1991). Some sources of friction factor uncertainty are the type of mud and its lubricity, cuttings bed, dogleg/keyseat, wellbore curvature, borehole torsion, wellbore tortuosity, viscous effects, borehole diameter, asperity between the drillstring and wellbore, and flexural stiffness of the string (Samuel, 2010). In this section, the effects of mud, drillstring, BHA, tortuosity, well path, downhole tools and pipe rocking on friction are reviewed in detail.

### 2.4.1 Drilling Agitator Systems (DAS)

The industry has recognized that excessive friction limits the driller's ability to transfer weight to the bit and maintain control over tooface when sliding. For this reason, friction reduction tools called Drilling Agitator Systems (DAS) were developed and have been in use since 2002 (Burnett et al, 2013). They are still one of the leading friction reduction technologies currently available.

Agitators are downhole tools that oscillate axially, reducing drag by breaking static friction. The DAS is comprised of a drilling agitator tool (DAT) and a shock tool (Figure 3). The DAT has a 1:2 positive displacement mud motor with a valve and bearing section at the edge matched against a concentric orifice (Alali et al., 2011). This setting produces

a pressure pulse when mud is pumped through the tool which compresses and decompresses springs in the shock tool, creating an axial oscillation which spreads to both sides of the DAS.

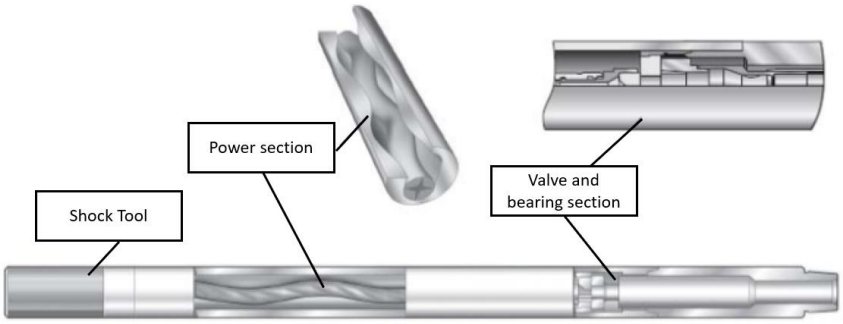


Figure 3: Scheme of a Drilling Agitator System (DAS). Modified from NOV, 2016.

An agitator typically causes a pressure drop of around 500-600 psi which must be accounted for in selecting mud pumps with increased pressure handling capacity. The pressure drop is transformed into an oscillation that spread throughout the drillstring and reduces friction accordingly.

Rasheed (2001) summarized the benefits of agitators as comprising extended PDC life, higher levels of WOB, reduced drill pipe compression, enhanced toolface control and increased rates of penetration. Many other successful applications have been reported in the literature since this tool became available (Skyles et al., 2012, Barton et al., 2011, Jones et al., 2016a). As Dykstra et al. (2001) and Falodun et al. (2005) show, in order to have a successful implementation of agitators, pre- and post-well planning are important to optimize well design.

A detailed analysis of agitator placement was done by Shor (2016). His work consisted in modeling the string as a combination of beam and mass-spring-damper elements. The effect of the agitator was simulated with a one-dimensional wave equation,

which captures the propagation of a harmonic excitation at angular frequency along a beam, and also includes damping. For DATs, the primary sources of damping are drillstring-borehole wall contact, viscous damping due to interaction with the drilling fluid, energy loss due to material hysteresis, and energy radiation into the formation.

With this model, it is possible to calculate the force at each node and compute the percentage of the drillstring that experiences enough force to overcome static friction. By iterating through a series of depth of interest, tool placement may be optimized. Figure 4 shows the percentage of the drillstring in dynamic friction as a function of bit depth and distance between the agitator and the bit for a horizontal well. This graph shows that locating the agitator farther away from the bit maximizes friction mitigation. This same model will be used later in this work to simulate pipe rocking.

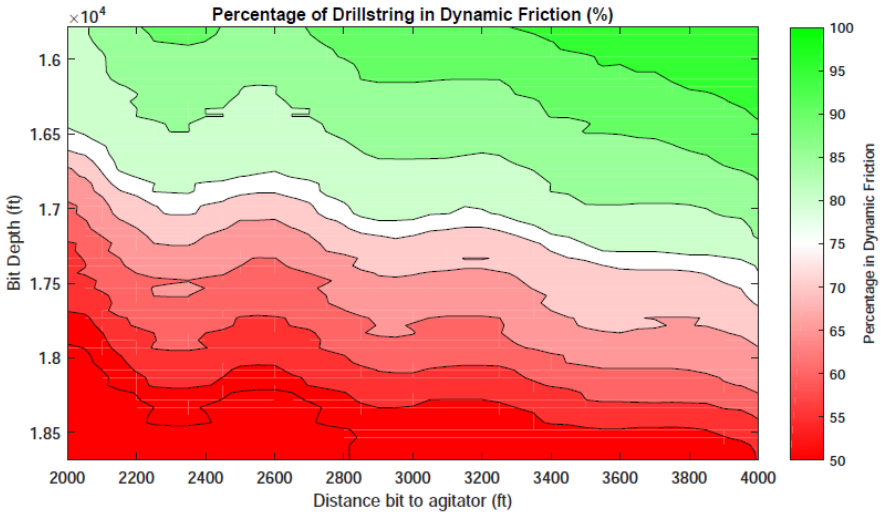


Figure 4: Location optimization of an axial oscillation tool in a horizontal well (Shor, 2016).

### 2.4.2 Pipe Rocking

Apart from the use of downhole tools, surface operations can be performed to reduce friction between the drillstring and the wellbore. Pipe rocking is a technique that has become popular in onshore directional drilling operations, mainly because it shows an improvement in the operation with little additional cost (Maidla et al., 2009). Rocking a pipe consists in creating torsional oscillations from the top drive, rotating the string alternately forward and backwards. This action breaks the static friction in a segment of the string, providing better toolface control and weight on bit (WOB) transfer during sliding operations (Gillan et al., 2009)

When rotation is applied at the surface, a torque wave propagates through the string. The shallower section of the string accumulates enough energy to break static friction and rotate. However, if the torque applied at the surface is not large enough, only a short segment of the string will be able to rotate while the rest will remain static. Consequently, only a part of the string would be under a dynamic friction regime. The depth at which the energy is not enough to rotate the string is termed as the maximum rocking depth.

Figure 5 shows a theoretical representation of how pipe rocking works. For explanation purposes, RPM is shown as a sinusoidal wave with an amplitude of 40 RPM and a period of 2 seconds. Under this regime, the top drive would rotate the top of the string a maximum of around 0.6 wraps in each direction.

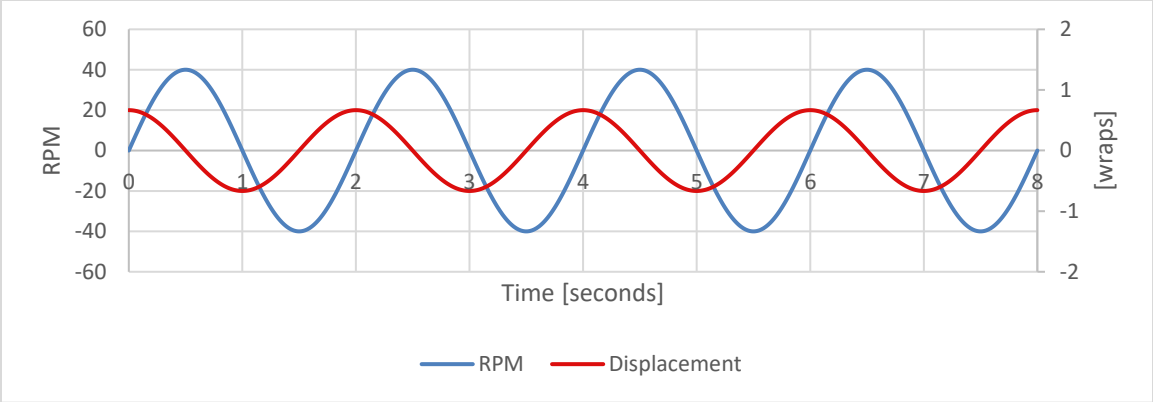


Figure 5: Representation of the theoretical behavior of top-drive RPM (Blue) and surface number of wraps (Red) during a pipe rocking regime.

Figure 6 shows a real pipe rocking example with surface RPM in blue and surface torque in green. Most data sources show absolute values for these parameters and so it is difficult to differentiate between forward and backward rotation. Another consideration that should be made when analyzing this pattern is that data from electronic drilling recorder (EDR) are generally sampled at one second at best. The change from positive to negative rotation can happen faster than that, and RPM is wrongly seen as a peak pointing downwards instead of going to zero. An interesting observation from this figure is that each period of rotation in one direction lasts for about ten seconds at fifty-five RPM. This means that the number of wraps or rocks in each direction is around nine.

Another interesting remark about Figure 6 is that torque builds up to a certain value until direction changes, it resets to almost zero and starts increasing again, but it never reaches a constant value. What this means is that full rotation is never achieved while rocking. This is a key parameter to controlling rocking operations and ensures a constant toolface during sliding operations. If surface torque is enough to break static friction in the whole string, the bit deviates from the desire direction and it must be reoriented.

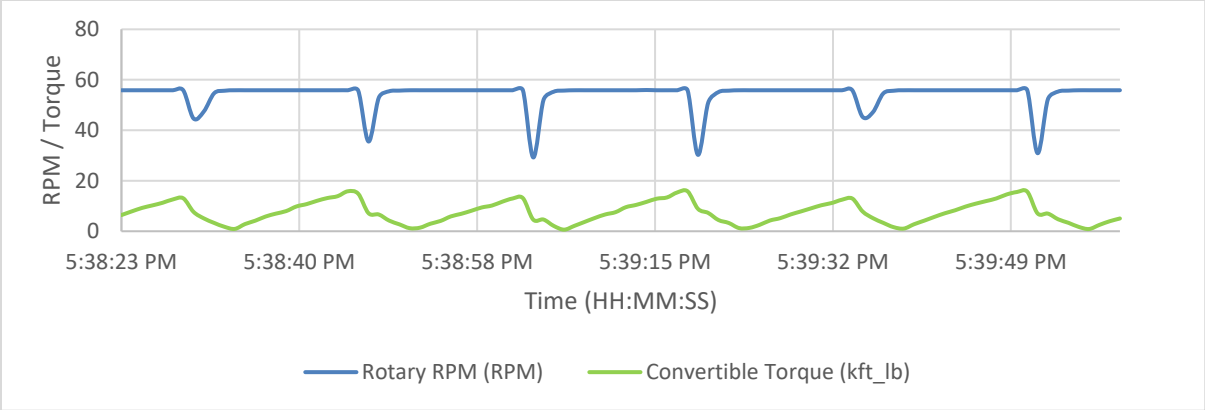


Figure 6: Real pipe rocking operation with Torque (green) and Rotary RPM (Blue). EDR data for this dataset is in absolute values.

Most rocking operations are still done manually in the field. An experienced directional driller estimates the number of wraps required to break enough static friction to have better WOB transfer and toolface control, without reaching full rotation. For each rocking interval, he or she counts the number of revolutions in one direction before turning into the other one. One of the goals of this thesis is to analyze this process and come up with an optimum rocking regime.

Rocking a pipe is a repetitive task that can take from a few minutes to a few hours, many times a day, making it an error-prone activity for humans. Possible errors during pipe rocking are twofold: either not rocking the pipe sufficiently or excessively rocking the pipe. Insufficient rocking of the pipe reduces maximization of the efficiency gains that are possible, while excessive rotation can lead to losing toolface orientation. Another concern is excessive rotation when spinning backwards (counter-clockwise). All drill pipes and downhole tools have connections designed to rotate clockwise when drilling, while counter-clockwise rotation can unscrew a connection. There is therefore a risk of disconnecting a connection while rocking backwards in what is called a back-off event. These have happened in the industry and will be studied in this thesis.

To maximize the effect of rocking and diminish the risk of such incidents, some companies came up with systems that have automated the pipe rocking process. Slider™ by Schlumberger and ROCKit™ by Nabors claim to provide significant improvements when slide drilling with their systems. These automated surface control systems intend to transfer weight to the bit without stalling the motor, reduce longitudinal drag to maintain a desired toolface and result in a higher ROP than with conventional sliding (Duplantis, 2016).

By considering standpipe pressure, differential pressure, hook load and MWD tool-face angle, Slider™ and ROCKit™ determine the amount of torque required to more efficiently transfer weight to the bit and keep a constant toolface. The driller or DD needs to set up the desired orientation and number of wraps in each direction and the automated system provides the surface torque and hook load to maintain this direction. While these systems can control the corrections needed to maintain a constant direction and oscillate the pipe automatically, the magnitude and frequency of torque pulses still needs to be input. In Slider™ the amount of torque in each direction needs to be provided as input, while ROCKit™ needs the number of wraps in each direction as an input (Figure 7).

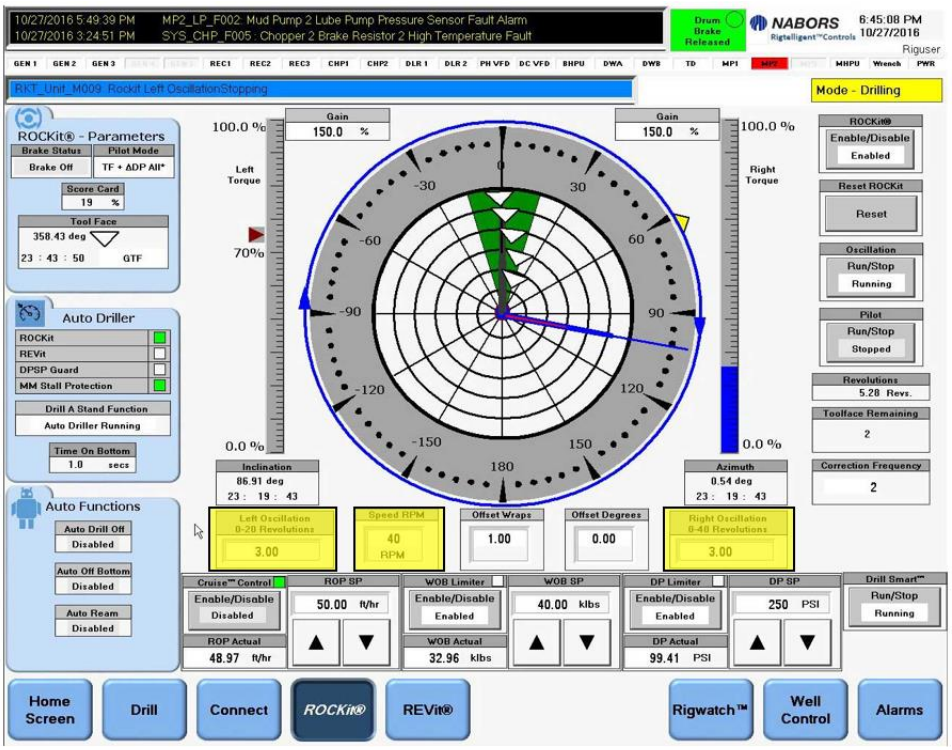


Figure 7: Screenshot of NABOR's ROCKit$^{TM}$ system. Highlighted in yellow are the values that need to be input by the driller to control the pipe oscillation regime (Modified from www.nabors.com, 2018).

As mentioned before, one of the main operational risks during pipe rocking are back-offs. All the elements in the string have connections designed to rotate clockwise. These connections have a designed make-up torque, which should be never reached during the entire operation, as an over-torqued connection may damage the threads, bringing additional drilling problems.

During pipe rocking, the top drive rotates the string counter-clockwise for small periods of time, and this can untwist or *back-off* a connection, meaning that the bottom part of the drillstring disconnects from the rest of the pipes. If this is the case, the driller may be able to make the connection again with clockwise rotation and reciprocating the string up and down until he or she sees an increase in hook load, meaning that the bottom part of

the string got attached. Even if this is accomplished, the driller should trip out to inspect all connections and make sure the drilling operation can proceed with all the joints coupled with the specified make-up torque. If the driller is not able to reconnect the missing string, a fishing operation is required to bring it back to surface.

In both cases, this is a time-consuming process that can take several days of a drilling operation, increasing the total cost of the well substantially.

### 2.4.3 Mud Program Design

A good summary of friction reducing practices was documented by Schamp et al. in 2016. They wrote about the lessons learnt from an operation of extended reach deviated wells (ERDW) in the Russian Far East, where they were experiencing high torque. Their selection of non-aqueous fluids (NAF) resulted in a 20%-40% reduction in friction against WBM, but this was not good enough for deeper wells. Solid or chemical fluid additives were then added to the mud to increase its lubricity. Solid lubricants act like ball or roller bearings between the drillstring and casing or wellbore, while chemical lubricants form a film between the two surfaces to minimize contact and consequently reduce the coefficient of friction.

When mixing liquid additives to OBM or SOBM, alteration of the drilling fluid rheological properties can be expected, especially to plastic viscosity and yield point. As an alternative, solid lubricants with different bases can be used in conjunction with liquid non-aqueous lubricants. Treated graphite powder with a liquid based lubricant has been documented to reduce the friction factor by half in horizontal drilling operations (Mohammadi et al., 2015).

The performance advantage of NAF compared to WBM is usually evident, but the savings resulting from higher ROP, shale inhibition and reduction in torque and drag is often undercut by the higher costs of NAF and environmental regulations. Efforts to reduce environmental footprint and the drilling costs of drilling with NAF have been reported since 1991, when Christiansen showed the negative impact the discharge of contaminated mud was having in the North Sea. He also showed that horizontal wells could be drilled with WBM without a significant change in torque, drag and rate of penetration if using appropriate additives. Since then, friction reducing formulations of WBM have been developed to replace the use of OBM.

Friedheim et al. showed a similar experience they had in 2003 in Deepwater Gulf of Mexico when designing a high-performance water-based mud (HPWBM). They were trying to drill with a water-based mud that had a similar composition to the one used in the North Sea, but it failed in completely inhibiting the hydration of highly water-sensitive clays, which in turn resulted in balling, accretion, wellbore instability and poor penetration rates. Instead, they designed a drilling fluid with three additional additives that would generate a triple inhibit effect in shale-hydration, dispersion and accretion.

HPWBM has also proved to match or outperform OBM in unconventional reservoir drilling as shown by Yadav et al. in 2015. The key to their success was to design a mud based on the mineral composition of cores and cutting samples that guaranteed shale stability, particle plugging, swelling and cutting integrity. They achieved these properties with the use of nano-size based materials to provide wellbore stability and shale control. Alshubbar et al. (2017) showed that nanoparticles of barite in a WBM can reduce friction by generating a smooth film that coats the surfaces.

Mechanical lubricants can also be added to WBM to reduce friction, as shown by Haddad et al. in 2017. In their work, they were able to reduce torque, pick-up and slack-

off factors respectively by 27%, 52% and 42%, and then drill the longest ERD well in the history of their operation in offshore Abu Dhabi with a final depth of 23,000 ft. They used an algae-based powder lubricant covered in a microscopic encapsulation. When enough pressure is applied to the encapsulations (i.e. when exposed to friction between surfaces), the cell membranes break and deploys lubricating oil that sticks to the rubbed surfaces.

When designing drilling mud, any combination of these additives needs to be tested to prove a reduction in friction for specific drilling conditions. Kaarstad et al. (2009) tested the effect of temperature on eight different lubricants and they observed that friction coefficient increased with temperature by 20% to 50% for all fluids but OBM. They also provided a linear relation between friction coefficient and temperature for different fluids, which can be used in torque and drag models. Figure 8 shows a range of friction factors for WBM, OBM and SOBM, with or without additives. Also, compatibility checks with the specific operation are needed, as for example solid fibrous lubricants may plug downhole tools. Finally, it needs to be noted that lubricants may not be the most cost-effective solution to decrease friction, they can be subject to environmental restrictions and may cause additional formation damage.

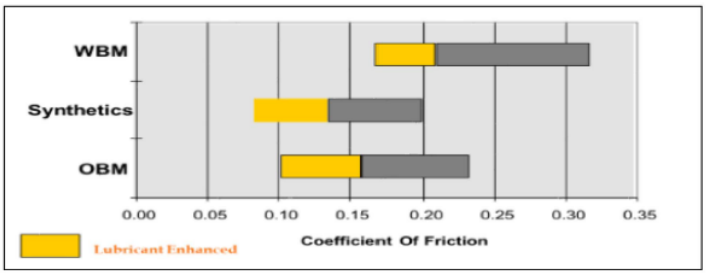


Figure 8: Typical friction factors for different drilling fluids and effect of lubricants. Haddad et al, 2017.

### 2.4.4 Effect of BHA and Drillstring Design

Mason et al. (2000) presented the benefits of placing roller-based subs (Figure 9) when drilling high-angle wells. Rollers have the function of reducing the contact area of the string against the wellbore and provide a sliding contact between the pipe and the borehole or casing.

Figure 9: Roller-based drilling sub. (Mason et al., 2000).

Placement of torque reducing tools is important as subs that are placed too close together can add stiffness to the string, inducing higher normal forces, and if they are too far apart, sagging of the tubular increases contacts with the wellbore, increasing friction. Yim et al. (2015) reported improved drilling efficiency with the use of torque reducing subs while drilling horizontal sections after a build section of 10°/30m for the curve, placing them every two joints for the BHA in contact with the lateral section. These proved effective in reducing surface torque and open hole friction factor by reducing the surface area in contact with the wellbore. Overall, the torque was reduced by almost 30% and

longer runs were achieved with lower damage to the bit comparing to drillstrings that do not use these subs.

As these tools have additional moving elements, it is important to evaluate the tools' robustness for the specific drilling operation to reduce the risk of losing parts in the hole. McCormick et al. (2011) summarized a series of improvements done to these subs after ten years of experience to increase their trustworthiness and versatility.

Another downhole tool was presented by Jones et al., 2016b. This tool is not meant for reducing friction, but rather to accommodate force transfer fluctuations at the bit. As maintaining constant WOB and DP can be challenging during slide drilling operations, they created a steady weight on bit tool (SWOBT) to maintain these parameters constant at the bit. The SWOBT changes its length in response to differential pressure changes at the positive displacement motor (PDM). It shortens its length with increases of torque in the PDM, while a decrease in torque causes the SWOBT to lengthen. After running several field trials, they concluded that the SWOBT can reduce the bit damage resulting from RPM variation and manage the negative effects to improve bit life to drill longer sections.

Drill pipe comprises most of the length of a drillstring and therefore its' selection also plays an important role in friction management. Range III drill pipes have a length of 13.5-14.8 m, while range II are between 9.2 m to 10.2 m. The additional length in between joints causes a larger contact area due to drill-pipe sagging in horizontal sections (estimated to be around seven meters for the longer pipes) and should be taken into consideration during the well construction planning phase.

Drill pipe internal diameter (ID) and outside diameter (OD) also play an important role in friction contribution. In general, a higher diameter drill pipe has a larger polar moment of inertia, which increases the torque needed to rotate it. Additionally, the resulting smaller clearance in the annulus leads to a higher risk of increasing drag due to the friction

between restrictions in the wellbore and the drill pipe. However, Hill et al. showed some of the benefits of increasing the ID and OD of the pipes. For such long drillstrings, high surface pump pressure is needed if smaller ID pipes are used. Turbulent flow is desired in the annulus and is achieved with a higher annular velocity, but this also requires higher pressures. Higher ID pipes allow for higher annular velocities at lower pressures. Another way to promote turbulent flow is reducing the annular area between the wellbore and the pipe, which can be done by increasing OD (Tomren et al., 1986). Lafuente et al. (2017) studied the findings of Hill and optimized drill pipes by specifically designing a 4-1/4", 15.40 lb/ft drill pipe for shale applications, which not only optimized the hydraulics for improved hole cleaning, but also decreased side forces a 40%, with a direct impact in drag reduction.

### 2.4.5 Hole Cleaning Best Practices

Poor hole cleaning generally results in higher torque and drag and is seen when hook load values deviate from regular torque and drag models, mainly by having higher than expected pick-up weights (Aarrestad et al., 1994). In high-angle wellbores, deficient hole cleaning is mainly evidenced in tripping out operations, when large OD BHA elements such as stabilizers tend to plow the cuttings beds accumulated on the bottom, causing high overpulls (Rasi, 1994). Overpulls are caused by the high friction of the drillstring with the cuttings in the wellbore. Additional friction due to poor hole cleaning has a negative impact on directional drilling operations, as weight transfer to the bit is less efficient. Additionally, due to the elastic nature of the string, a larger OD tool can be partially stuck in a cutting bed and break free when enough weight is applied to it. This will cause a sudden weight release against the formation, and this can damage the bit and stall a downhole motor.

Rasi (1994) described the problem of hole cleaning in high-angle wells, including horizontal wells, as the effect of cuttings falling to the lower side of the hole because of gravity and forming a cutting bed. This is not a big concern while rotating the string but can be problematic during tripping or sliding drilling operations. It is then necessary to both, minimize the height of the cuttings bed that forms while drilling and reduce the tendency of the drills string components to plow the bed and form plugs of cuttings.

Tomren et al. (1983) studied the phenomenon of cuttings accumulation in deviated wells with a test section, a section of pipe in a lab. They analyzed the effect of fluid annular velocity, hole inclination, fluid rheological properties, penetration rate, pipe/hole eccentricity, drill pipe rotary speed, and pipe/hole diameter ratio. They observed that bed of cuttings started to accumulate at inclinations greater than 40° and this increased with lower flow rate. Between 35° and 55°, bed forms and slides downward against the flow, so when circulation is interrupted the annulus content moves down quickly. At higher angles, a reduction in the cuttings bed is achieved by having turbulent flow in the annulus, independently of the fluid viscosity. They observed that turbulent flow can be reached mainly at high annular velocities and at the same time, Brett et al. (1989) and Guild et al. (1993 and 1994) showed the importance of drill pipe rotation for lifting the particles from the lower side of the wellbore. They also noticed that reciprocating the drillstring up and down considerably helps cuttings transport.

In 1995 Guild et al. showed how these concepts were put in practice in an extended reach well hole cleaning program in an operation in the U.K. First, they monitored torque and drag during the operation by registering pick-up, slack-off and rotating off bottom hook-loads on each connection. Then, they would contrast the values obtained against the predicted weight modeled with Johancsik's theory, allowing the driller's awareness of downhole conditions. A divergence of pick up and slack off weights indicates that the hole

is being loaded with cuttings, while convergence is a sign of the hole being cleaned up. If cuttings start loading on the lower side of the wellbore, reciprocation, rotation and circulation until pick-up weight decreases and slack-off weight increases is needed.

Many empirical and mathematical methods were developed to calculate the minimum flow rate needed for cleaning the cuttings out of the well (Larsen et al., 1997, Bizanti et al., 2003, Malekzadeh et al 2011). These models are functions of hole diameter, pipe size, angle of deviation, plastic fluid viscosity, yield point, mud weight, cutting specific gravity and the rate of penetration. In their experience, they found that annular velocities of 4.5 to 5 ft/s are needed to have proper hole cleaning in holes with deviations greater than 50°. Ravi et al. (2006) showed that pipe eccentricity has a positive effect in this phenomenon.

Zhang et al. developed a simulator in 2017 to study the transient solid transport of cuttings to revise commonly used rules of thumb practices and the effect on torque and drag. One of their motivations was to analyze the increase in ECD given the high flow rates required by previously described models. They recommended to stop drilling and circulate more frequently as the lateral length increases. This circulation should be thorough, with at least four bottoms-up in long laterals.

Naganawa et al. (2017) took a step forward with a transient cuttings-transports simulator that accounts for the effect of wellbore tortuosity. A tortuous path can lead to trapping of a cuttings be in a trough of the well, leading to a reduced cleaning action. Local cuttings accumulation on downtips reduce cleaning action, increasing friction and the risk of having a stuck pipe.

### 2.4.6 Planned Tortuosity, Large-Scale Tortuosity and Micro-Tortuosity

Tortuosity generally follows an inverse relation with wellbore quality. A smooth, frictionless finish, in-gauge hole that follows the original directional plan can be referred as a 'perfect wellbore'. Benefits of such a wellbore would be minimal torque and drag levels, drilling with minimal mechanical loads, improved weight transfer, easier hole cleaning, low vibrations, problem-free casing runs, etc. (Mason et al., 2005).

Tortuosity can be described as the amount by which the wellbore deviates from the planned trajectory (Gaynor et al, 2001). One main source of tortuosity is the 'slide/drill/slide' nature of directionally drilling with steerable motors and this is referred as large-scale tortuosity. Additionally, micro-tortuosity is often referred to as deviations in which the hole axis is a spiral instead of a straight line, forming small scale borehole spiraling. This type of tortuosity happens both with steerable motors and with RSS Systems (Gaynor et al., 2002) and are usually associated with vibrations and drill bit design. Total tortuosity can be divided into planned tortuosity, large scale tortuosity and micro tortuosity.

Wijermans et al. (2001) showed the benefits of drilling with a rotary steerable system over downhole motors, concluding that tortuosity is reduced not only in curved sections but also in tangent sections. They observed an increase of 28% in torque in tangent sections of those wells drilled with a steerable motor over those drilled with a rotary steerable system. Gaynor et al. (2002), analyzed torque and drag data from 100 wells in the North Sea drilled with downhole motors, steerable systems and slickbore systems (known for drilling with minimum hole spiraling). In addition to the findings like that of Wijermans et al. (2001), they attributed a decrease in friction factors from 0.27 to 0.21 in WBM and 0.12 to 0.1 in OBM to the minimizing of spiraling when using slickbore systems.

Brands et al. (2012) proposed a method to quantify the borehole undulations in terms of hole curvature, clearance and pipe stiffness, and studied the effect on torque and

drag. A highly tortuous well forces the pipe to bend along the contact points and when an axial load is applied, the pipe bends further due to the axial bending moments the force generates. This forces the pipe to adopt a more curved position, and with the increase in axial load, the pipe uses the peaks and valleys to compress, resulting in a higher pipe curvature than the wellbore curvature. An increase in side forces generates more friction against the wellbore. They simulated this effect with a stiff-string torque and drag model with contact points to properly represent the tortuosity effect on drillstring deformation (Figure 10). With this theory, they obtained an expected higher friction in lower clearance scenarios, as well as in cases with increasing amplitude (maximum variation of angle over the planned survey) or frequency. Periods of 5-15 ft correspond to micro-tortuosity, while longer periods of 100-500 ft correspond to large scale tortuosity (Menand, 2013).

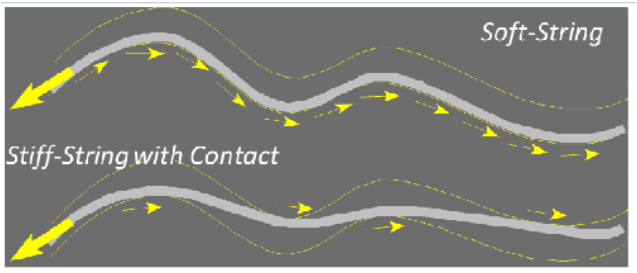


Figure 10: Differences in soft-string and stiff-string with contact torque and drag models. The latter is needed to properly model effect of tortuosity on friction. (Menand, 2013).

As surveys from MWD are usually taken every 90 ft, these cannot be reliably used to measure micro-tortuosity (Figure 11). Micro-tortuosity can be a source of increase in torque and drag that is invisible to regular surveying techniques; masked micro-doglegs that lead to distorted friction factors can yield erroneous interpretation of downhole conditions. Lowdon et al. (2015) presented the advantages of using high-resolution survey instead to properly quantify tortuosity. By using scaling techniques, they were able to

identify which curvatures in the well can create tight spots and which ones are benign. Caliper, borehole imaging and wire logs are another way to measure micro-tortuosity in the wellbore.

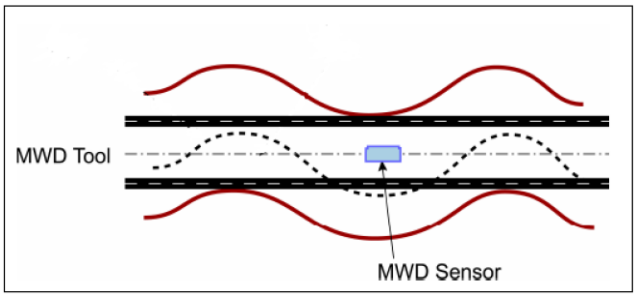


Figure 11: Scheme of micro-tortuosity and position of MWD. MWD survey tool cannot measure a tight spiral (Gaynor et al, 2002).

Large-scale and micro-scale tortuosity are a result of the nature of drilling tools and the operation itself. However, the third component of tortuosity, planned tortuosity, can be minimized during the early stages of well planning.

### 2.4.7 Directional Plan Design

The work from Fontentot (1973) was one of the first ones to present excessive torque and drag due to directional plan in an operation in the Gulf of Mexico. In their operation, it was needed to rapidly build and then drop angle to follow the contour of a salt dome. They created a parameter to quantify the hole shape, developed to describe the effect of hole angle and depth. As expected, higher values of torque correlated with those wells that had higher hole shape parameters. By considering torque and drag during the early stages of well planning, a directional well can be designed to minimize friction due to planned tortuosity.

A complete study of the shape effect of extended reach wells (ERW) on torque and drag in sliding, rotary and tripping modes was done by Ma et al. in 1998. Their main goal was to minimize torque and drag by modifying the well trajectory in wells with long horizontal departure and high inclination. They analyzed nine types of well shapes in build sections and found that those with lower frictions had sideway catenary curves, curvature-decreasing curves and circular arcs.

For tangent sections, Liu and Samuel (2009) proposed that there is a critical angle up to which the drillstring slides downwards by gravity action (Equation 1). Hence, tangent sections with an inclination below the critical angle are desired to minimize drag. This angle is a function of the friction factor and hence can be altered by implementing friction reducing practices considered in the early stages of well construction.

$$\alpha_{cr} = tan^{-1}\left(\frac{1}{\mu}\right) \quad \textbf{(1)}$$

In unconventional projects, directional plan is usually constrained by the extent of the play area and the requirement to maximize the horizontal section to be hydraulically fracked. Curves are built by maximizing DLS with the available downhole tools. Torque and drag models must be run in advance to guarantee that the proposed directional planned is feasible. In this scenario, all the elements that affect the friction factor can be revised to have a successful drilling job. For example, the use of additional downhole tools for friction reduction has become popular in unconventional drilling operations to more effectively reach planned total depth (TD).

## 2.5 Literature Review Conclusions

Friction has remained one of the main challenges to deal with when drilling highly deviated wells. Some of the main problems that high friction produce are: reduction in

rotary and sliding ROP, high tortuosity, inferior wellbore quality, premature downhole tools and bit damage, drilling dysfunctions such as vibrations and back-offs, shorter wells and stuck pipes. For this reason, every aspect of drilling a well should be reviewed in order to reduce friction.

Drilling fluid has a major influence on friction. Non-aqueous fluids usually have lower friction coefficient than WBM. However, much more can be done apart from choosing the right base. Chemical and mechanical additives can help reduce friction even more. In some cases, it has been shown that WBM, with the proper additives outperform NAFs.

Roller-based tools can be placed along the drillstring to provide a rolling transition between the string and the wellbore. However, other components of the BHA and the drillstring can increase friction. Although high OD tools such as stabilizers reduce the clearance to the wellbore and therefore facilitate turbulent flow, they tend to producer higher friction against the wellbore and their use should be limited. Additionally, higher OD pipes have a larger moment of inertia and then higher torque is needed to rotate them.

A hole cleaning program is mandatory and should be specifically designed for each inclination and set of tools to prevent a bed of cuttings from accumulating in the lower section of the hole. Special attention should be given to highly tortuous wells, as cuttings can accumulate in downtips along the wellbore.

Tortuosity acts as another source of friction. Large scale tortuosity is a consequence of drilling with a sliding technique and produces an increase in torque and drag. This may be reduced with the use of RSSs, which drill a much smoother well. However, even these tools produce micro-scale tortuosity, which is a spiraling along the axis of the well. This is invisible to conventional MWD measurements and can account for a significant increase in drag. The third type of tortuosity, planned tortuosity, can be anticipated by running a

torque and drag model in advanced. From studies, it has been found that the type of curves that minimize friction for 3D wells are catenary curves, curvature-decreasing curves and circular arcs.

Finally, another way to mitigate friction is to force a dynamic regime in sections of the string that usually slide against the wellbore. By adding an oscillatory tool that produces small axial displacements, part of the string breaks static friction. The farther the tool is placed from the bit, the higher this effect. Additionally, torsional oscillations can be generated from surface to break static friction in the shallower section of the well producing a similar effect.

# Chapter 3: Physical Models for Pipe Rocking

The goal of pipe rocking modeling is to find a robust methodology that provides the driller with recommendations on an optimum rocking regime, consisting of the number of wraps and the RPM at which the pipe should be oscillated to minimize friction. The solution to the problem described here was found by combining a torque and drag model with a torsional damped wave equation. In this chapter, these two models are explained in detail.

## 3.1 TORQUE AND DRAG MODEL

Johancsik et al. (1984) summarized the main causes for excessive torque and drag as being tight hole conditions, sloughing holes, keyseats, differential sticking, cuttings buildup caused by poor hole cleaning, and sliding wellbore friction. They were the first to calculate and quantify the effects of torque and drag while tripping with no rotation or rotating off bottom. Since then, many other models were developed to consider combinations of rotation and tripping (Tveitdal, 2011). Later on, stiff string models with different types of interactions between the pipe and the wellbore wall were also developed (Aslaksen et al., 2006). However, the original model proved to work well in many scenarios and is still used in many commercial software (Mitchell et al., 2007).

The basic premise of this model is that torque and drag forces in a directional well are caused mainly by sliding friction, which is typically calculated as the product of the sidewall contact force with the friction factor (FF). While friction coefficients are approximated from experimental data, the contact force can be calculated analytically. There are four outputs estimated using this model for various depths:

(1) The hook load when the drillstring is static (static weight); (2) the hook load when the drillstring is tripped in (slack-off weight); (3) the hook load when the

drillstring is tripped out of hole (pick-up weight); (4) the torque when rotating off-bottom (free rotating torque).

When calculating these values, friction is assumed to be caused entirely by sliding friction forces between the string and the hole. The string is divided into segments and the final torque and drag values are obtained as the sum of the individual contributions on each segment. A free body diagram for an arbitrary segment during a picking up operation is shown in Figure 12. There are 5 forces acting on this segment:

1. The weight of the segment ($W$) in the vertical direction
2. The normal force on the segment ($Fn$) perpendicular to the contact point between the string and the wall
3. The tension on the lower side ($Ft$) parallel to the string with a certain azimuth ($\alpha$) and inclination ($\theta$),
4. The tension on the upper side ($Ft + \Delta Ft$) parallel to the string with another azimuth ($\alpha + \Delta\alpha$) and inclination ($\theta + \Delta\theta$)
5. The friction force ($Ff$) acting in the direction opposite to the pipe's direction of movement, calculated as the product of the normal force and the FF ($\mu$).

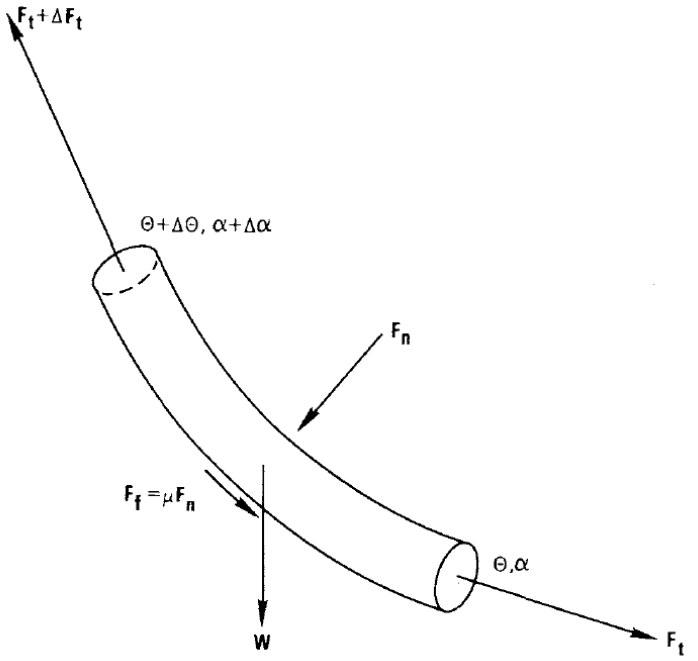


Figure 12: Free body diagram of a drillstring segment during a picking up operation (Johancsik et al., 1984).

To obtain the normal force, all forces are assumed to act on the center point of the segment and are decomposed into orthogonal components. Figure 13 shows how the forces can be decomposed if the string is lying in a vertical plane (2D). Vector analysis yields the magnitude of the normal force (Equation 2), where $\bar{\theta}$ is the average of the inclinations at the beginning and the end of the segment (Equation 3).

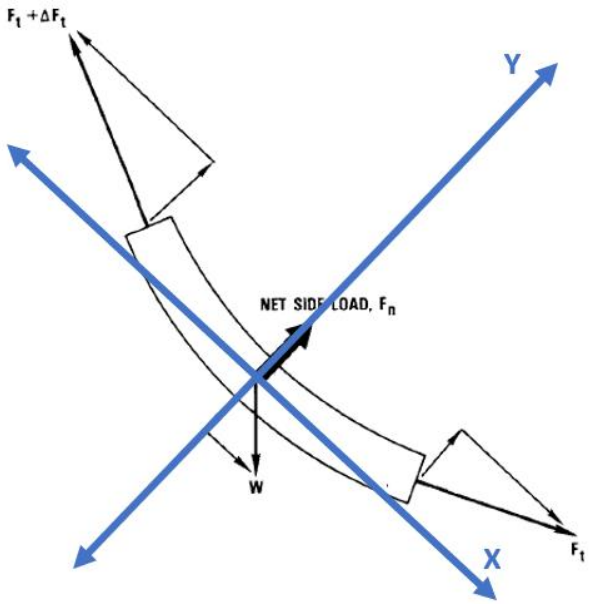


Figure 13: Force balance for the drillstring segment (Modified from Johancsik et al, 1984).

$$F_n = \sqrt{(F_t \, \Delta\alpha \, sin\bar{\theta})^2 + (F_t \, \Delta\theta + W \, sin\bar{\theta})^2} \quad (2)$$

$$\bar{\theta} = \frac{\theta_1 + \theta_2}{2} \quad (3)$$

The tension at the top of the segment can be obtained from the tension at the bottom of the segment plus the weight of the segment, plus the friction force contribution of the segment (Equation 4). If the string is static, the last term is set to zero. When tripping out, the term is positive, and when tripping into the hole, the term is negative.

$$F_t + \Delta F_t = F_t + W cos\bar{\theta} \pm \mu \, F_n \quad (4)$$

To simplify the calculations, Equation 4 is usually re-written with available parameters in a regular drilling operation. Consider an arbitrary segment as the one in Figure 14, with bottom and top measured depths, inclinations, and azimuths $MD_1$, $MD_2$, $\theta_1$,

$\theta_2$, $\alpha_1$ and $\alpha_2$, respectively. Equations 5 and 6 show the reformulation of Equation 4 in these parameters. In these equations, *w* represents the unit weight of the segment, *OD* the outer diameter of the segment, $\rho$ the mud density and $\rho_{st}$ the density of steel.


Figure 14: Arbitrary drillstring segment.

$$F_n = \sqrt{\left[F_t \frac{|\alpha_1 - \alpha_2|}{(MD_1 - MD_2)} sin(\bar{\theta})\right]^2 + \left[F_t \frac{|\theta_1 - \theta_2|}{(MD_1 - MD_2)} + w(MD_1 - MD_2)(1 - \frac{\rho}{\rho_{st}})sin(\bar{\theta})\right]^2} \quad \textbf{(5)}$$

$$\Delta F_t = w(MD_1 - MD_2)(1 - \frac{\rho}{\rho_{st}})cos(\bar{\theta}) \pm \mu F_n \quad \textbf{(6)}$$

Finally, the expected tension load at a segment is calculated as the weight at the bottom of the string ($F_o$) plus all the individual tension increments up to that segment (Equation 7). The tension load at the surface is then $F_o$ plus the contributions of all the *N* segments into which the string is divided (Equation 8). $F_o$ is usually assumed to be zero if the string is off-bottom.

$$F_{t,i} = F_o + \sum_{r=0}^{i} \Delta F_{t,r} \quad (7)$$

$$F_{t,Hook\ Load} = F_o + \sum_{r=0}^{N} \Delta F_{t,r} \quad (8)$$

The torsional increment can be obtained by multiplying the friction force by the radius of the segment, as done in Equation 9, and the expected surface torque is calculated using Equation 10, where $M_o$ is the torque at the bottom of the string, usually assumed to be zero when the string is off-bottom.

$$\Delta M = \mu F_n \frac{OD}{2} \quad (9)$$

$$M_{surface} = M_o + \sum_{r=0}^{N} \Delta M_r \quad (10)$$

First, for a given drillstring configuration and a given directional survey, Equations 8 and 10 are used to estimate static, slack-off and pick-up weights and surface torque with the bit assumed to be on bottom with no WOB. Next, the string is assumed to be lifted a small distance (e.g. 30 ft), and the calculations are repeated. This process is repeated until the bit reaches the surface and the result is an estimation of the expected hook loads and torque during tripping out and tripping in operations. These values are used to check if the rig has the capacity to perform these operations. This model is run with different FFs, and real data can be superimposed on the modeled results to find the FF that best matches the observations. The work by Maidla and Wojtanowicz (1990) can be used to estimate the difference in the FFs for rough and smooth surfaces (i.e. borehole wall and casing).

Figure 15 shows the results of applying Johancsik's model to a horizontal well with the last casing string set at 8,300' and kick-off-point (KOP) at 8,500'. Pick-up and slack-off weights and torque are simulated for FFs varying from 0.1 to 0.5. The blue dots in the

drag graph represent the operational pick-up data. It can be seen that the model predicts the observations quite accurately for a FF of 0.2.

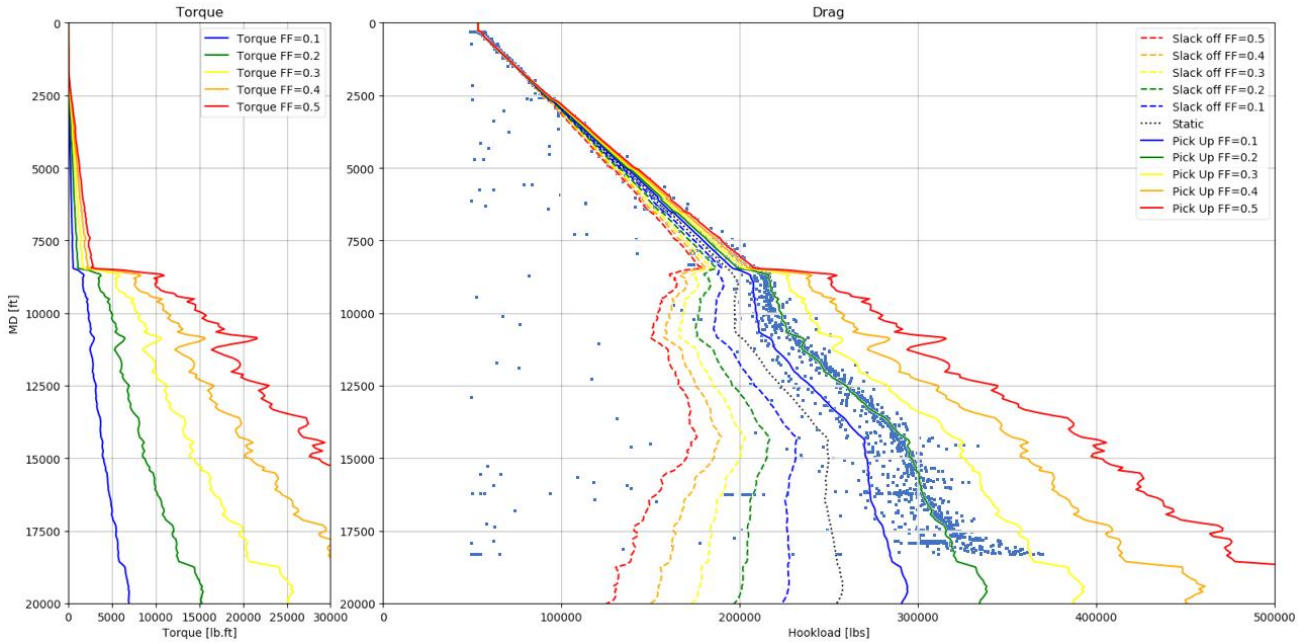


Figure 15: Example of Johancsik's torque and drag model applied on a horizontal well.

It is to be noted that when the string is almost at surface (i.e. measured depth close to zero), the expected hook load is not zero. This is because the sensors also measure the weight of the hook and block, which is typically obtained from the data set and added to Equation 8.

### 3.2 Damped Wave Equation

A damped wave is a wave whose amplitude gradually decreases over time. One good example of a damped wave is the oscillation generated on water surface when a rock is thrown in it. A wave propagates on the surface and decreases its amplitude over time and

distance until it reaches equilibrium once again. Only one-dimensional propagation is considered here for pipe rocking. Equation 11 represent the 1-D undampened wave equation, where $\psi(x,t)$ is the wave function and $v$ the characteristic phase velocity (Fitzpatrick, 2013). A damping term dependent on the velocity of the wave can be added to obtain the one-dimensional damped wave equation (Equation 12).

$$\frac{\partial^2 \psi}{\partial t^2} = v^2 \frac{\partial^2 \psi}{\partial x^2} \tag{11}$$

$$\frac{\partial^2 \psi}{\partial t^2} = v^2 \frac{\partial^2 \psi}{\partial x^2} - c\frac{\partial \psi}{\partial t} \tag{12}$$

Several missing constants are needed to model the drillstring dynamics during pipe rocking operations. Shor (2016) derived the damped wave equation for axial drillstring oscillations. A similar approach was taken to get the torsional damped wave equation. The angular form of Hooke's law gives the relation between applied torque and angular deformation (Equation 13), where $T$ is the torque applied, $J$ is the polar moment of inertia, $G$ is the shear modulus, $\tau_{\emptyset z}$ is the shear stress, $\gamma_{\emptyset z}$ is the shear strain, $z$ is measured depth and $t$ represents time.

$$\frac{T}{J} = \tau_{\emptyset z} = G\gamma_{\emptyset z} = G\frac{\partial \emptyset}{\partial z} \tag{13}$$

An increase in force is related to the acceleration of an incremental mass according to Newton's law (Equation 14).

$$\frac{\partial T}{\partial z} = \rho J \frac{\partial^2 \emptyset}{\partial t^2} \tag{14}$$

Equations 13 and 14 can be combined to obtain Equation 15, which can be rewritten as Equation 16.

$$\frac{\partial}{\partial z}\left(GJ\frac{\partial \emptyset}{\partial z}\right) = \frac{\partial T}{\partial z} = \rho J\frac{\partial^2 \emptyset}{\partial t^2} \quad \textbf{(15)}$$

$$\frac{\partial^2 \emptyset(z,t)}{\partial t^2} = \frac{G}{\rho}\frac{\partial^2 \emptyset(z,t)}{\partial z^2} \quad \textbf{(16)}$$

Considering that the torsional wave velocity is defined as in Equation 17, the torsional undamped wave equation is finally obtained as in Equation 18, which depends on the drillstring physical properties.

$$v_t = \sqrt{\frac{G}{\rho}} \quad \textbf{(17)}$$

$$\frac{\partial^2 \emptyset(z,t)}{\partial t^2} = v_t^2\frac{\partial^2 \emptyset(z,t)}{\partial z^2} \quad \textbf{(18)}$$

As in Equation 12, damping is added with a velocity-dependent term that removes torque displacement as shown in Equation 19.

$$\frac{\partial T}{\partial z} = \rho J\frac{\partial^2 \emptyset}{\partial t^2} - C\frac{\partial \emptyset}{\partial t} \quad \textbf{(19)}$$

The damping coefficient can be rewritten as in Equation 20, and finally the torsional damped wave equation is obtained (Equation 21).

$$c = c(z,t) = \frac{C}{GJ} \quad \textbf{(20)}$$

$$\frac{\partial^2 \emptyset(z,t)}{\partial t^2} = v_t^2\frac{\partial^2 \emptyset(z,t)}{\partial z^2} - c\frac{\partial \emptyset}{\partial t} \quad \textbf{(21)}$$

The latter equation is dependent on the drillstring configuration ($v_t$) and on a certain constant "*c*", the damping coefficient. The four main sources of damping are (see e.g.Shor, 2016): (1) material hysteresis, (2) friction with the borehole, (3) viscous friction with the borehole fluids, and (4) radiation of energy into the formation. For the model discussed here, it is assumed that of these sources friction with the wellbore is the dominant one, and others can be ignored. Shor obtained the damping factor (*C*) for Coulomb friction by calculating the work done in an axial oscillation cycle and this is used to calculate the angular damping factor.

The work done in an axial oscillation (one full upwards and downwards displacement cycle) can be calculated by integrating the Friction force (Equation 22), which is rewritten as in Equation 23, and the differential *dz* is rewritten as Equation 24.

$$\boldsymbol{W = \int F_f dz} \tag{22}$$

$$\boldsymbol{F_f = C\frac{dz}{dt}} \tag{23}$$

$$\boldsymbol{dz = \left(\frac{dz}{dt}\right) dt} \tag{24}$$

A harmonic motion with maximum amplitude *X* at steady state is described by Equation 25. Finally, for a complete cycle, the integral can be rewritten as shown in Equation 26.

$$\boldsymbol{z = Xsin(\omega t - \emptyset)} \tag{25}$$

$$\boldsymbol{W = \int_0^{\frac{2\pi}{\omega}} \left(C\frac{dz}{dt}\right)\left(\frac{dz}{dt}dt\right) = C\omega^2 X^2 \int_0^{\frac{2\pi}{\omega}} cos^2(\omega t - \emptyset)dt = \pi C\omega X^2} \tag{26}$$

By considering that the work done is the force times distance ($W=F_fX$), the damping factor can be found as in Equation 27, where $F_n$ is the normal force obtained from Johancsik's model as in Equation 5.

$$C_{axial} = \frac{F_f}{\pi\omega X} = \frac{\mu F_n}{\pi\omega X} \quad (27)$$

Finally, the precedent equation is transformed to get the damping factor for torsional oscillations. The frequency is replaced with the RPM, and the maximum axial displacement is replaced with a maximum angular displacement, defined as a maximum angle $\emptyset_{max}$, times the radius of the element (Equation 28).

$$C_{angular} = \frac{\mu F_n}{\pi RPM \emptyset_{max} r} \quad (28)$$

By coupling together the normal force (Equation 5), the torsional damped wave equation (Equation 21) and damping factor (Equation 28), a pipe rocking model is created that is dependent on the drillstring configuration, the wellbore geometry, the drilling mud and the pipe rocking regime.

### 3.3 Finite Difference Approximation

The equations obtained in the previous section can be used to solve for the angular displacement of a single segment in the drillstring. To simulate the behavior of the whole string, the finite difference approximation method is used. The first step is to approximate the derivatives from Equation 21 using central differences, as shown in Equations 29, 30 and 31 (Shor, 2016). In these equations *i* represents discretization in space and *n* is the discretization in time.

$$\frac{\partial \emptyset(z,t)}{\partial t} \approx \frac{\emptyset_i^{n+1} - \emptyset_i^n}{\Delta t} \tag{29}$$

$$\frac{\partial^2 \emptyset(z,t)}{\partial t^2} \approx \frac{\emptyset_i^{n+1} - 2\emptyset_i^n + \emptyset_i^{n-1}}{\Delta t^2} \tag{30}$$

$$\frac{\partial^2 \emptyset(z,t)}{\partial z^2} \approx \frac{\emptyset_{i+1}^n - 2\emptyset_i^n + \emptyset_{i-1}^n}{\Delta z^2} \tag{31}$$

With these approximations, Equation 21 can be rewritten as Equation 32.

$$\frac{\emptyset_i^{n+1} - 2\emptyset_i^n + \emptyset_i^{n-1}}{\Delta t^2} = v_t^2 \frac{\emptyset_{i+1}^n - 2\emptyset_i^n + \emptyset_{i-1}^n}{\Delta z^2} - c\frac{\emptyset_i^{n+1} - \emptyset_i^n}{\Delta t} \tag{32}$$

$$\emptyset_i^{n+1} = \frac{1}{1 + c\Delta t}\left[\frac{\Delta t^2 v_t^2}{\Delta z^2}(\emptyset_{i+1}^n - 2\emptyset_i^n + \emptyset_{i-1}^n) + (2 + c\Delta t)\emptyset_i^n - \emptyset_i^{n-1}\right] \tag{33}$$

Following the equations of motion, boundary conditions are defined to run the model as follows. The angular displacement of the drillstring on surface matches the regime imposed at the top drive, which for a rocking operation can be described by Equation 34. This signal generates rotation of the string in each direction for a *T* period of time, at an angular velocity $RPM_{set}$.

$$RPM_{surf} = sgn\left[cos(\frac{\pi t}{T})\right] RPM_{set} \frac{2\pi}{60} \tag{34}$$

At the bottom of the string a free boundary condition is set (Equation 35). This means that the bit rotates freely with no interaction with the formation. While this is strictly not true for actual drilling operations, it does fit the purpose of the simulation.

$$\emptyset_{bit}^n = \emptyset_{bit}^{n-1} + \left(\emptyset_{bit-1}^n - \emptyset_{bit-1}^{n-1}\right) \tag{35}$$

The string can be divided into three sections when performing pipe rocking (Figure 16): the first section from the surface to the maximum rocking depth, the second section

from the maximum rocking depth to the point of interference, and the thirs section from the point of interference to the bit (Duplantis, 2016). In the first section, the string rotates and there is dynamic friction between the string and the wellbore. On the next section, there is pure sliding between the drillstring and the formation. In the section that goes from the point of interference to the bit (called the "zone of influence"), the static friction broken by the vibrations caused by reactive torque can produce vibrations that break the static friction. The simulator has the option to consider the effect of reactive torque or not depending on the level of vibrations. If these are minimal, the model can disregard the effect of reactive torque and just analyze the rotary propagation from the surface down to the point of interference.

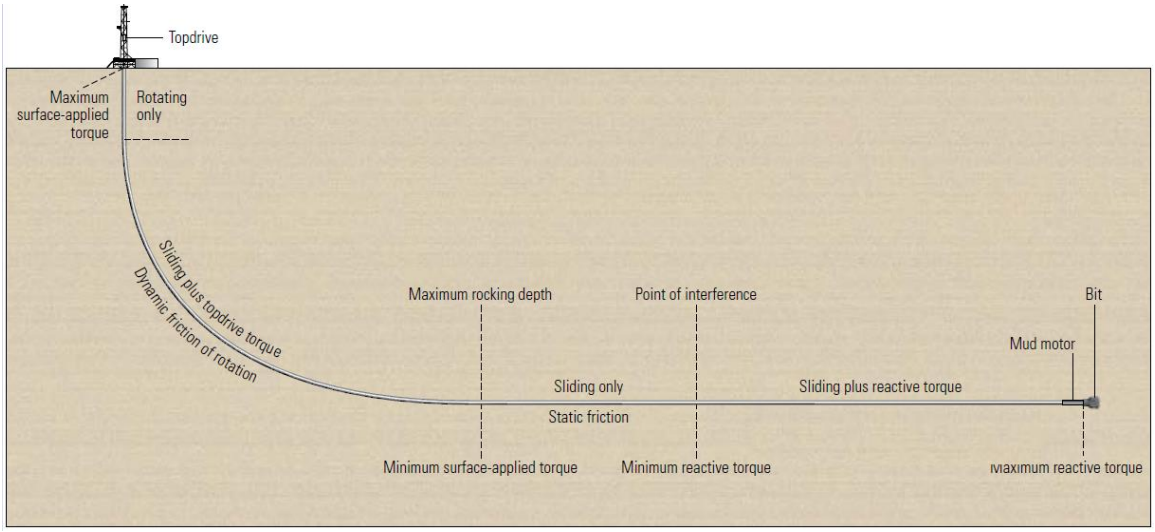


Figure 16: Sliding and dynamic friction in different sections of the drillstring during pipe rocking (modified from Duplantis, 2016).

If downhole vibrations break static friction in the lower section of the well, the simulator works as follows.

1. The section between the point of interference and the bit is considered to have a FF of zero, meaning that there is no restriction of movement downwards of the point of interference. This also implies that if the rotational wave reaches the point of interference, the drillstring will immediately rotate across its entire length.
2. The length of the zone of interference is assumed to increase linearly with the reactive torque at the bit. A reactive torque constant (RTC) is introduced to relate the depth of the point of interference with the reactive torque (Equation 36).

$$\boldsymbol{MD_{Point\ of\ interference} = TD - Tq_{reactive} * RTC} \quad \textbf{(36)}$$

Reactive torque is assumed to be the torque at the mud motor. Equations 37 to 39 adopted from Mitchell et al. (2011) can be used to calculate the mud motor's torque.

$$\boldsymbol{HP = \frac{\eta \Delta p Q}{1714}} \quad \textbf{(37)}$$

$$\boldsymbol{N = \frac{231Q}{Ap_r n_r}} \quad \textbf{(38)}$$

$$\boldsymbol{T = \frac{5,252HP}{N}} \quad \textbf{(39)}$$

where differential pressure $\Delta p$ is in psi, flow rate $Q$ in gal/min, bit rotational speed $N$ in rev/min and the cross-sectional area of the flow path $A$ in in$^2$. $p_r$ si the rotor pitch, $n_r$ the number of lobes in the stator and $\eta$ the mud motor's efficiency. Mathematically, the torsional damped wave equation simulates a transfer of energy from one segment to the other, even when this amount of energy is minimal. In reality, a minimum amount of energy needs to be transferred to break static friction. To model this phenomenon, in order to produce an angular displacement in a segment, the angular velocity of it needs to be higher than a minimum $RPM_{min}$. If this condition is not met, this segment remains static for this time step as shown in the flow chart in Figure 17.

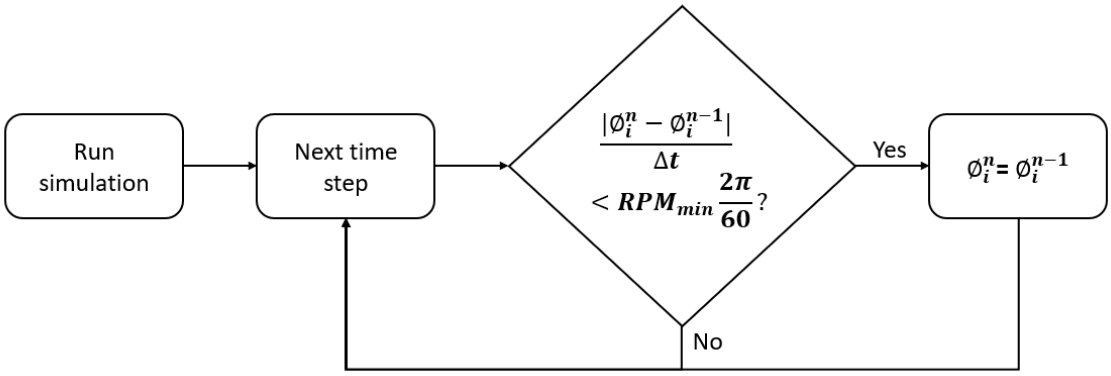


Figure 17: Flow chart for determining if a segment is static or in motion.

Some considerations need to be made when implementing the pipe rocking simulator. The main challenge is to convert available BHA and surveys data to a finite number of segnts with their required properties: length, ID, OD, unit weight, polar moment of inertia, inclination, and azimuth. Both BHA configurations and surveys are usually available in excel or pdf files, with values varying according to the string used and the number of surveys taken during the operation. For this reason, the first section of the code consists of taking the available data and transforming it to the predefined *N* finite elements chosen for the simulation.

The second section of the code is dedicated to calculating the normal force, tension and damping coefficient for each segment. Finally, the damped wave equation is solved for each time step and segment. For the simulation to be stable, the time required for the wave to propagate across a segment should be higher than a time step (i.e., a wave cannot "jump" an segment from one time step to the other). The time step is chosen to be half the wave propagation time through a single segment (Equation 40).

$$\Delta t = \frac{\Delta x}{2v} = \frac{L}{2N}\sqrt{\frac{\rho}{G}} \quad \textbf{(40)}$$

### 3.3.1 Determination of Constants

Most of the variables involved in the pipe rocking simulator can be obtained from available drilling data: pipe length, OD, ID, unit weight, mud weight, well survey, etc. However, the model also needs the determination of the damping factor *C*, which is used to calibrate the simulations. This value is constant for each segment, and is dependent on the segment's radius, friction force and $Ø_{max}$, which is also assumed to be the same for all finite elements.

The most precise way to obtain $Ø_{max}$ is from real data. Two methods to calibrate the model are from the torque signal and from downhole data. Figure 18 shows what the expected torque should be when surface rotation is applied to the string (Maidla et al, 2004). From points *a* to *b*, the string only rotates in a fraction of the string. From point b up to full rotation, toolface rotates with a different angular speed than the top drive or rotary table for some time, until the whole strings rotates at the set RPM. From point *a* to full rotation, energy travels along the string. This information can be used to calibrate the model.

The time needed for the torque signal to stabilize is recorded. Then, iterative simulations are done, adjusting $Ø_{max}$ until the time required for the drillstring to reach full rotary mode in the simulation matches the previously recorded value. Figure 19 shows an example of a well being drilled at 18,700 ft, for which it took approximately 15 seconds to reach full rotation at 70 RPM.

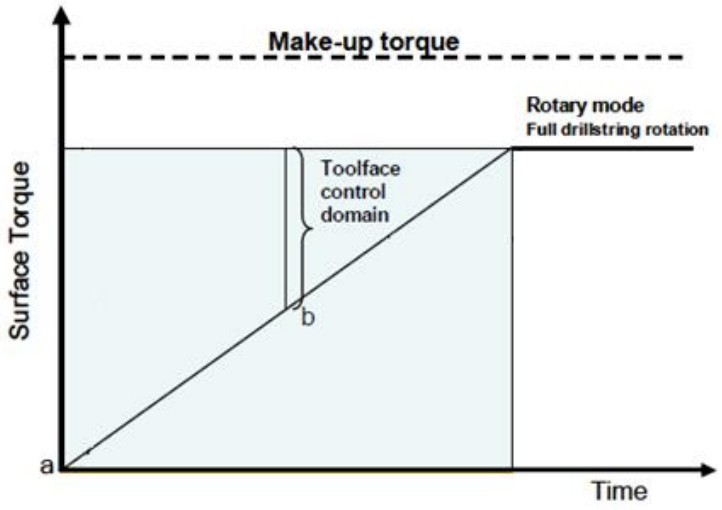


Figure 18: Surface torque as a function of time (Adapted from Maidla et al, 2004).

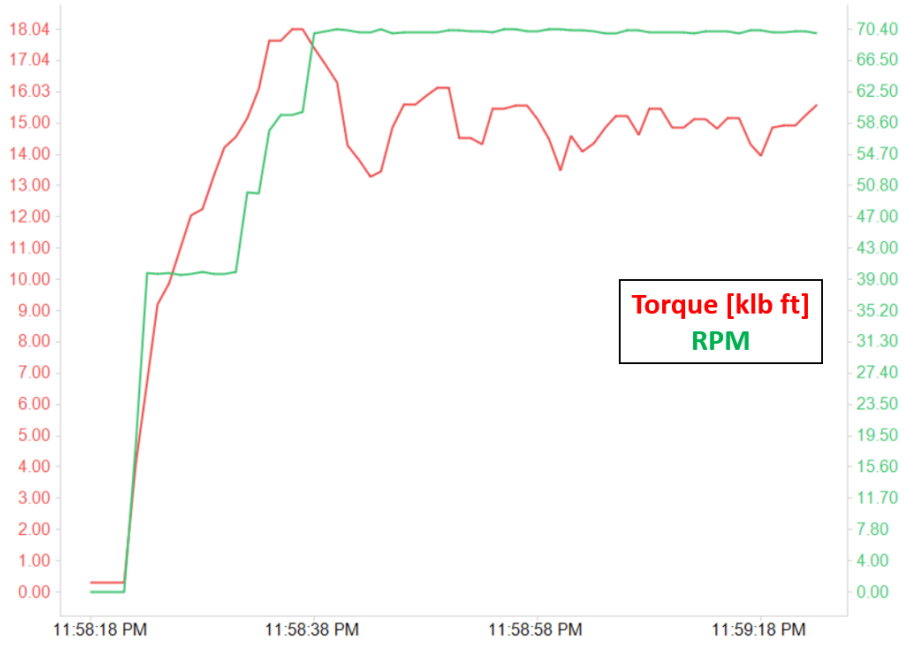


Figure 19: Torque signal from a real operation when applying 70 RPM from surface to a 18640 ft well.

The model can be even more precisely calibrated with downhole data. Downhole sensors give precise information on the RPM at a certain depth during the operation.

However, this data is usually stored in memory and only retrieved at the surface after the BHA run (meaning that the calibration cannot be done in real time). If downhole data is available in real-time, $\emptyset_{max}$ can be altered so the model represents the downhole conditions accurately. Table 1 summarizes the pros and cons of the different methods described to calibrate the pipe rocking simulator.

The maximum angular displacement in a time step $\emptyset_{max}$ can be calculated analytically when no additional information is available, as in Equation 41. This equation should only be used when no other information is available. The real maximum angular displacement is expected to be smaller, because only the segments on surface are expected to rotate at the RPM set by the top drive.

$$\emptyset_{max} = \frac{\boldsymbol{RPM}}{\boldsymbol{60}} \boldsymbol{2\pi\Delta t} \tag{41}$$

| Method | Pros | Cons |
|---|---|---|
| **Mathematical** | • Always possible<br>• Can be obtained in real time<br>• Calculation is instantaneous | • It may not represent the real field scenario |
| **From Torque signal** | • Can be obtained in real time<br>• Represents the real field scenario relatively well | • Torque signal may not reach a constant value<br>• Calculation is not instantaneous (≈15 sec) |
| **From downhole data** | • It represents accurately the real field scenario | • Not available in all wells<br>• Even when available it is typically not real time<br>• Calculation is not instantaneous (≈15 sec) |

Table 1: Pros and cons of different methods to calibrate the pipe rocking simulator.

# Chapter 4: Rocking Data Analytics

Transforming the pure sliding motion of the drillstring during slide drilling to a dynamic one along a major portion of the drillstring has helped directional drillers maintain better toolface control and drill faster. However, there are no industry guidelines on an optimum pipe rocking regime. The goal of this chapter is to use the models described in the previous chapter and perform multiple simulations to arrive at recommendations on pipe rocking regimes.

## 4.1 Pipe Rocking Simulator Outputs

The horizontal well detailed in Table 2 and shown in Figure 20, taken from a real field example, was used for the purpose of simulations described in this chapter. Figure 21 shows the outputs obtained after running a simulation rocking at 30 RPM and 6-second intervals for 3.5 seconds. The graph at the top of Figure 21 shows the number of turns along the drillstring and the one at the the bottom shows the RPM at each segment. At this particular instant in time, the surface pipe has rotated 3 seconds forwards and 0.5 seconds backwards, and will continue to rotate for another 5.5 seconds before changing the direction again. Notice that the first rotation is carried out for only half a cycle, to ensure that the string rotates around the initial state, and not only in one direction.

| | |
|---|---|
| ***Type of well*** | Horizontal |
| ***Drill Pipe*** | 4 ½', 16.6 lb/ft |
| ***HWDP*** | 54 joints, 4 ¾', 54 lb/ft |
| ***Mud density*** | 9.4 ppg |
| ***Initial departure*** | 2,000 ft |
| ***KOP*** | 8,500 ft |
| ***TD*** | 16,000 ft |

Table 2: Well information for initial simulation

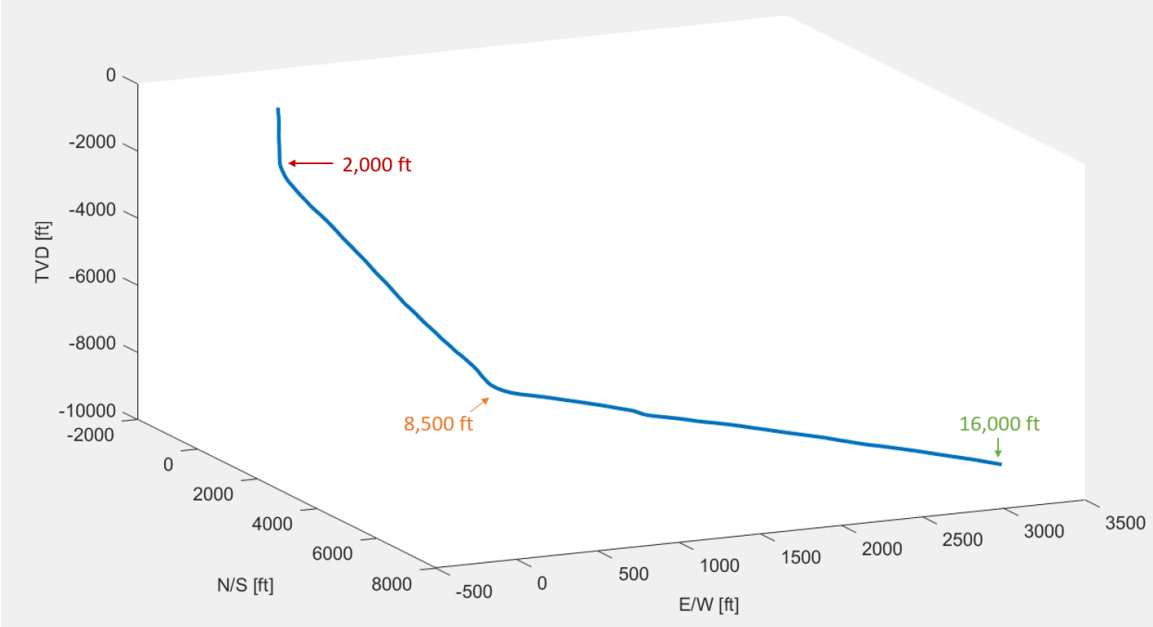


Figure 20: Horizontal well with vertical departure at 2,000 ft MD and KOP at 8,500 ft MD, during a pipe rocking operation at 16,000ft MD.

Figure 21 shows that the rotation at the surface does not reach the bottom of the well (green line). In fact, the rotation decreases substantially from the first departure point (red line – 2,000 ft) to the KOP (orange line – 8,500 ft). From the KOP onwards, the dissipated energy decreases even more due to the higher friction against the wellbore in the horizontal section. The maximum rocking depth is in the lateral section at around 10,500 ft MD as indicated by the black arrow in the figure.

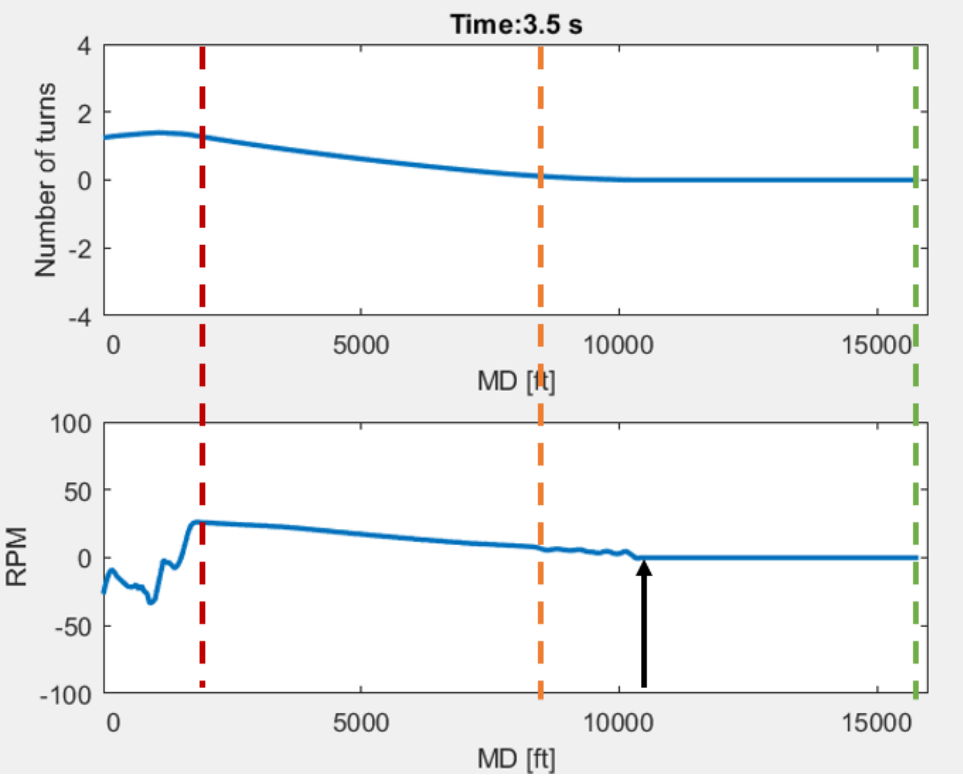


Figure 21: Number of turns and RPM of the segments in the drillstring as a function of measure depths, rocking at 30 RPM on 6 second intervals, after 3.5 seconds of simulation.

The maximum rocking depth is obtained for each time step in the simulation by looking for the last segment in the drillstring (from the bottom) that remains static. Figure 22 shows the maximum rocking depth as a function of time for this same operation. The black arrows point to the maximum rocking depth at 3.5 seconds, which matches the one from Figure 21. This figure shows that the rotation is transmitted fast until the KOP (8,500 ft) is reached. From this point onwards, where the friction against the wellbore is higher, it takes a longer period of time to propagate to the depth of the maximum rocking depth. This depth increases until the wave from the backwards rotation reaches the wave from the previous cycle, producing a sudden decrease of the fraction of string with dynamic motion.

This happens at approximately 9 seconds after the beginning of this particular simulation. After that, the cycle repeats, matching the period used in the rocking regime. In this case, the period is 6 seconds, as indicated by the reversals and associated reduction in maximum rocking depth observed at 9, 15 and 21 seconds. It should be noted that some of the fluctuations in the graph are due to the nature of the finite element simulation.

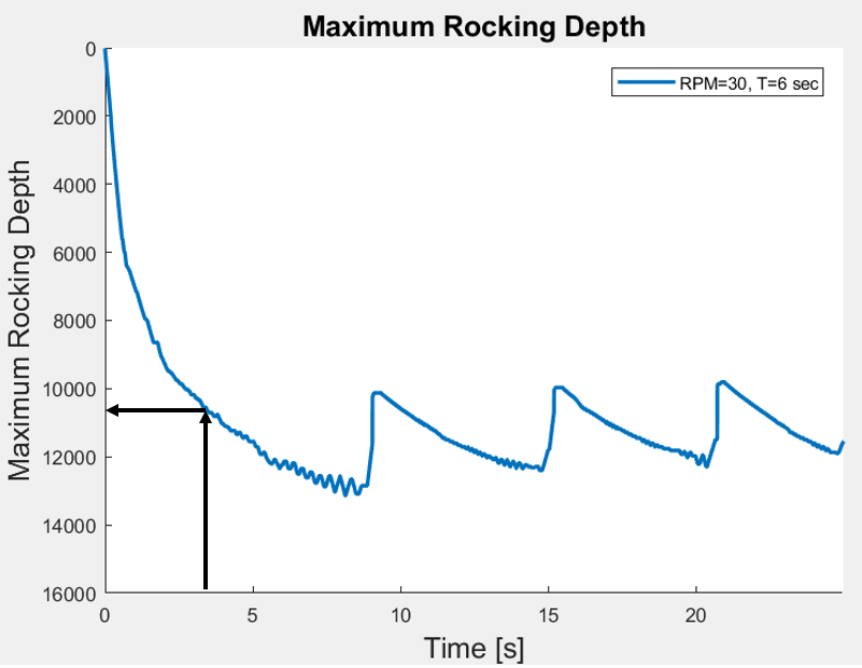


Figure 22: Maximum rocking depth over time for 25 seconds of simulation.

Figure 23 shows an example of how reactive torque can produce premature full rotation of the drillstring. For the same well previously described, the rocking regime in this simulation is changed to 50 RPM at 10-second intervals. Additionally, reactive torque is considered, and this results in dynamic friction in the deepest section of the drillstring. The simulation is run considering a maximum reactive torque of 2,000 lb-ft and a RTC of 150 ft/100lb-ft. Finally, instead of the maximum rocking depth, the fraction of the

drillstring under dynamic friction is shown on the y axis. In this simulation, there are moments during which 100% of the drillstring is in state of dynamic friction, meaning that rotation has reached the bit and a reorienting process is required.

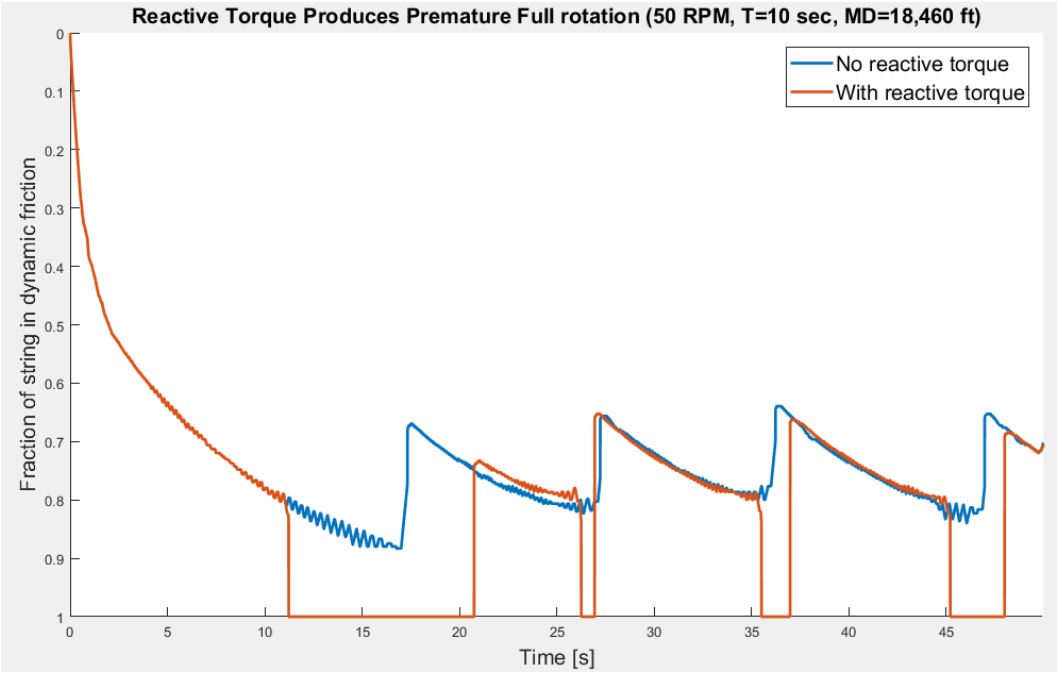


Figure 23: Reactive torque produces premature full rotation of the string. This rocking regime is unsuccessful when reactive torque is considered.

### 4.2 SIMULATOR CALIBRATION

Before it can be used for performing pipe rocking data analytics, the simulator needs to be calibrated for the well under consideration. A first attempt to calibrate the simulator was done by using downhole measurements. We illustrate the methodology using a well for which such data is available. Table 4 shows the information of this well. Both surface and downhole RPM were available only for a short section of the well. The downhole sub is situated 2,700 ft above the bit. A sliding segment with rocking was detected at 16,780 ft MD. Figure 24 shows that the downhole RPM during this rocking event was 0 when the pipe was being oscillated at 30 RPM in 19 seconds intervals. As it is challenging to see the change in direction in this graph, the rocking regime was obtained by visually looking at the raw data.

| | |
|---|---|
| ***Type of well*** | Horizontal |
| ***Drill Pipe*** | 4 ½', 16.6 lb/ft |
| ***HWDP*** | 54 joints, 4 ¾', 54 lb/ft |
| ***Mud density*** | 8.1 ppg |
| ***Initial departure*** | 1,900 ft |
| ***KOP*** | 8,200 ft |
| ***Downhole sub*** | 14,050 ft |
| ***TD*** | 18,640 ft |

Table 3: Well information for proceeding simulations

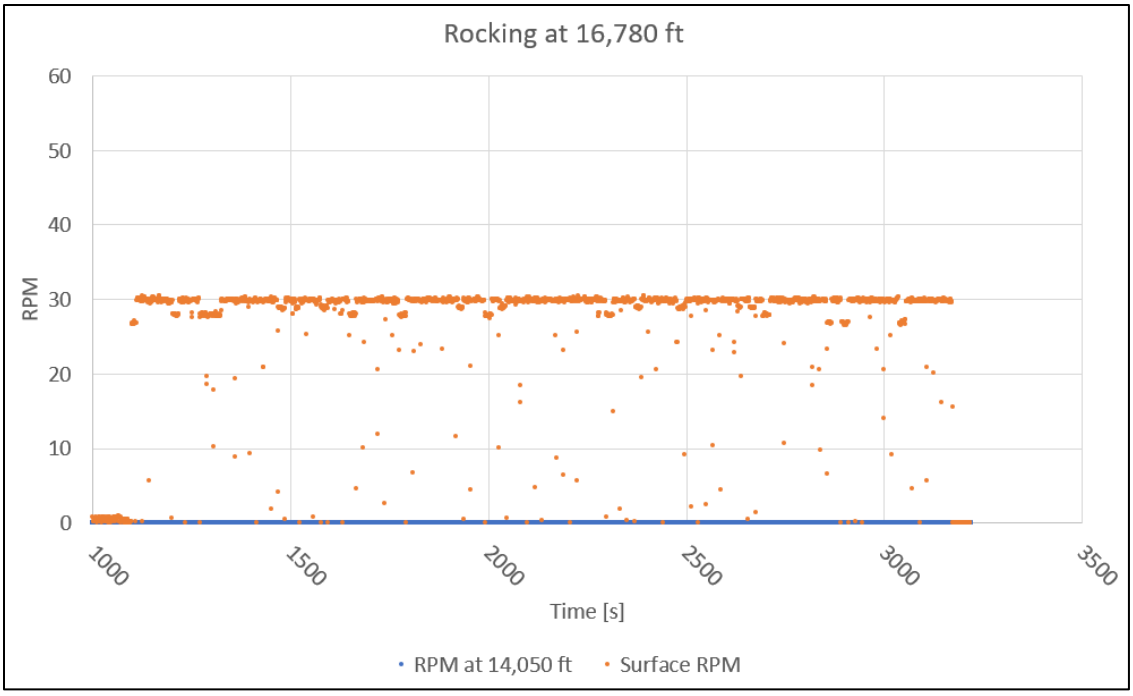


Figure 24: Surface and downhole RPM for a horizontal well during a rocking operation at 16,780 ft.

For this method, $Ø_{max}$ was adjusted until the RPM at the depth of the downhole sub matched that of the observed in the data, which in this case was 0 RPM (Figure 25). The secondary vertical axis shows the RPM at the depth of the sensor. In this case, it is assumed that the maximum rocking depth matches the sensor's depth. Most likely, that maximum rocking depth is shallower. For this method to be precise, the RPM measured downhole should be greater than zero. For this reason, a second calibration is attempted using the surface torque signal, described next.

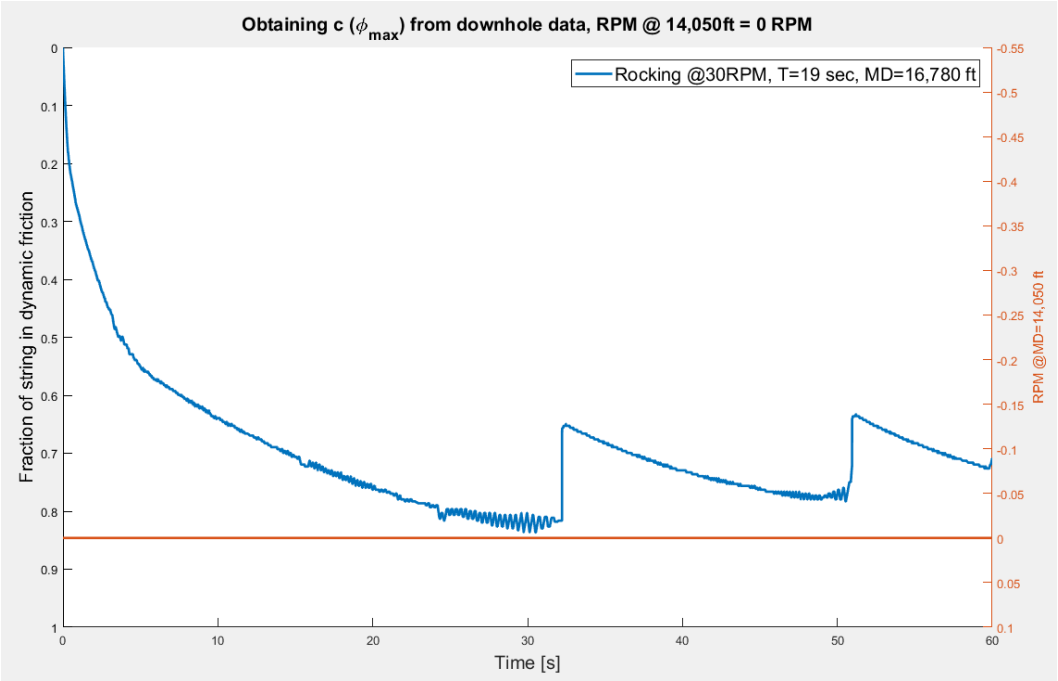


Figure 25: Model calibrated with downhole data. As the downhole sensor does not record any rotation at all, the calibration is not optimal.

Figure 26 shows the torque signal for the same well at the depth of 18,640 ft. In this example, the surface RPM is set at 70, and it takes 15 seconds for the torque signal to stabilize. Iterative simulations are done to find the value of $Ø_{max}$ that achieves full rotary mode at 70 RPM after 15 seconds, as explained in the previous chapter. Figure 27 shows the result of this calibration, which is considered satisfactory to perform data analytics of rocking operations on this well.

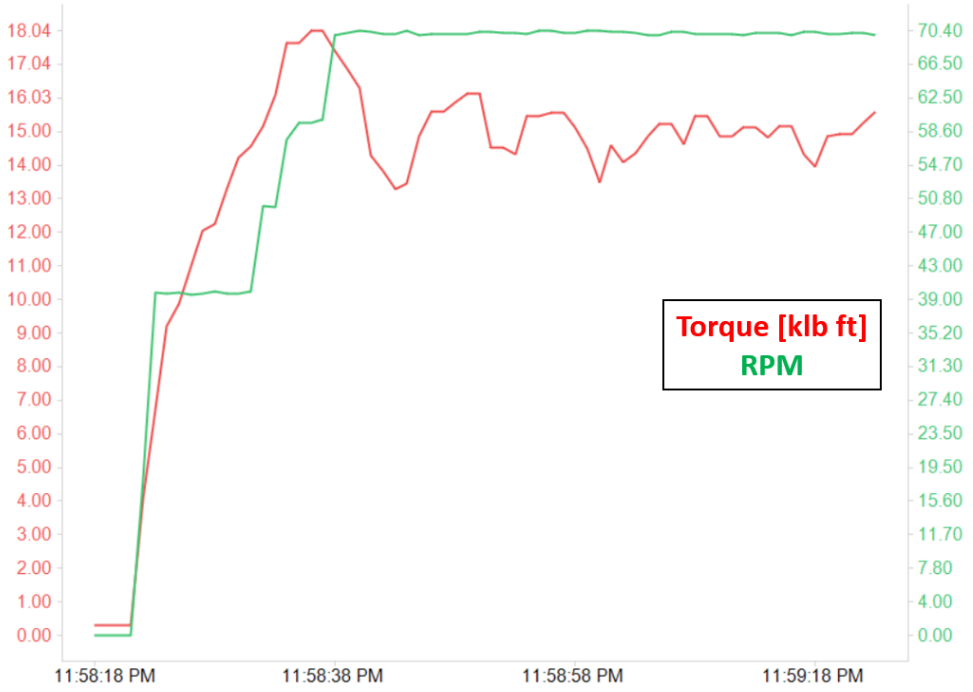


Figure 26: Torque signal from a real operation when applying 70 RPM from surface to a 18,640 ft well.

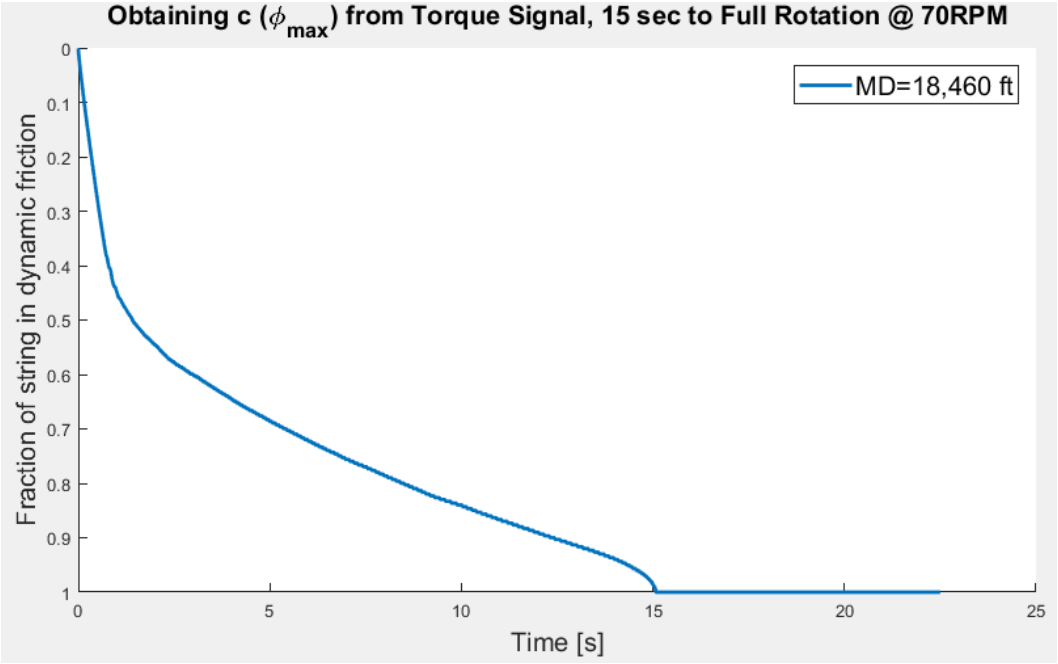


Figure 27: Simulator calibration from torque signal.

## 4.3 Pipe Rocking Data Analytics

The previously described simulator can be used to explore different rocking regimes and find the one that minimizes friction without placing the entire drillstring in a state of full rotation. Lower friction is expected when a larger fraction of the drillstring is under dynamic friction. The optimum rocking regime is expected to allow faster, easier and better sliding as discussed in previous chapters.

### 4.3.1 Friction Factor Variation

An initial simulation was done with a dynamic FF of 0.25 for the cased section and 0.32 for the open hole. Figure 28 shows a calibrated simulation for rocking at the deepest section of the well at 40 RPM in 5-second periods. A lower FF of 0.15 for the cases section (blue line) allows for better torque transfer, with a maximum of 79% of the string under dynamic friction, in contrast to only a maximum of 68% for a FF of 0.35 (green line).

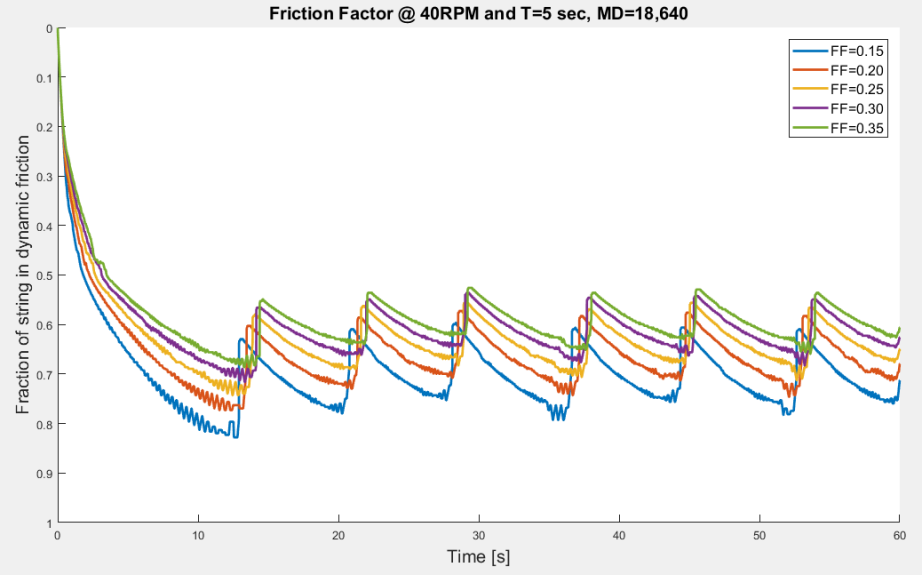


Figure 28: Effect of FF in pipe rocking.

### 4.3.2 RPM Variation

There are two main parameters that are controlled from surface during pipe rocking: the RPM and the period of oscillation. Figure 29 shows that with the period kept constant, a higher RPM causes a deeper maximum rocking depth. This result is expected, because the number of turns for the same period is higher in the cases with higher RPM. The effect is more noticeable in the vertical section where the normal force is lower. The separation between the lines for 10 RPM, 20 RPM and 30 RPM is higher than for the rest of the simulations. The first two RPM values have maximum rocking depth that do not reach the kick of point in this particular scenario. For an RPM of 30 (blue line), only 34% of the drillstring gets to rotate, while up to 80% of the string breaks static friction at 70 RPM (brown line).

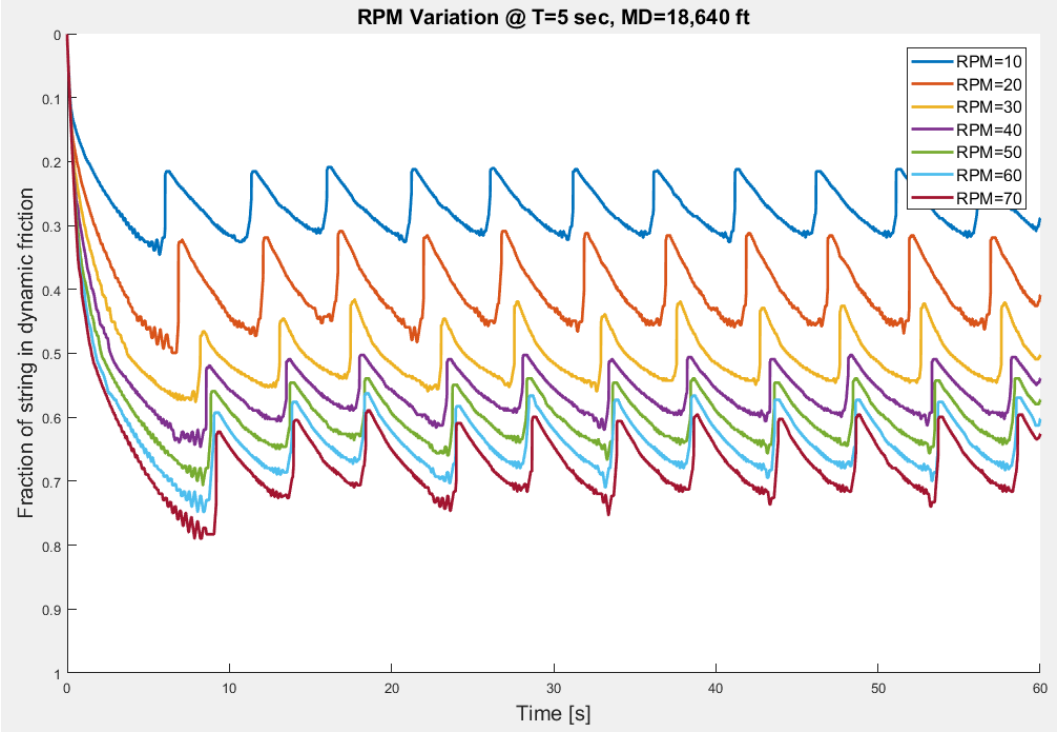


Figure 29:Effect of RPM in pipe rocking.

### 4.3.3 Period Variation

The next set of simulations was done at 40 RPM with different periods of rotation in each direction. Figure 30 shows that all the lines follow the same initial trend, but those with shorter time periods reach a shallower maximum rocking depth, because in these cases the number of turns in each direction is fewer. With short periods of only 2 seconds (dark blue), the rocking depth reaches 48% of the drillstring, but extends to 85% with 12 second cycles (light blue).

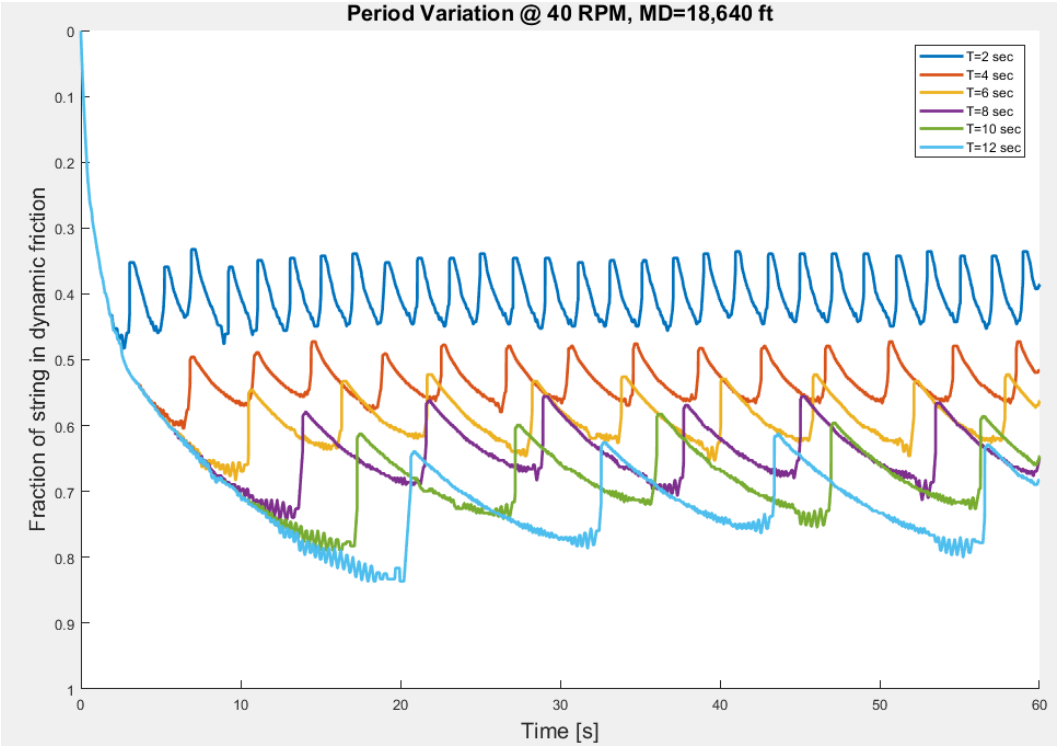


Figure 30: Effect of period in pipe rocking.

### 4.3.4 Regime Variation

As expected, increasing the RPM or the period of rotation increases the maximum rocking depth, which in turn allows for better force transfer to the bit and better and faster

slide drilling. Figure 31 shows six simulations in which RPM was increased from 20 to 70 by 10 RPM increments, adjusting the period of time so as to have the same the number of rotations to each side. In this scenario, after 20 seconds all the simulations yield similar results, with rocking depth varying between 60% to 80% of the string for all cases. The difference is in the transition between the minimum to the maximum depth, because those with higher RPM and lower period go faster from one state to the other, yielding an average maximum rocking depth slightly higher than those cases with lower RPM and longer periods.

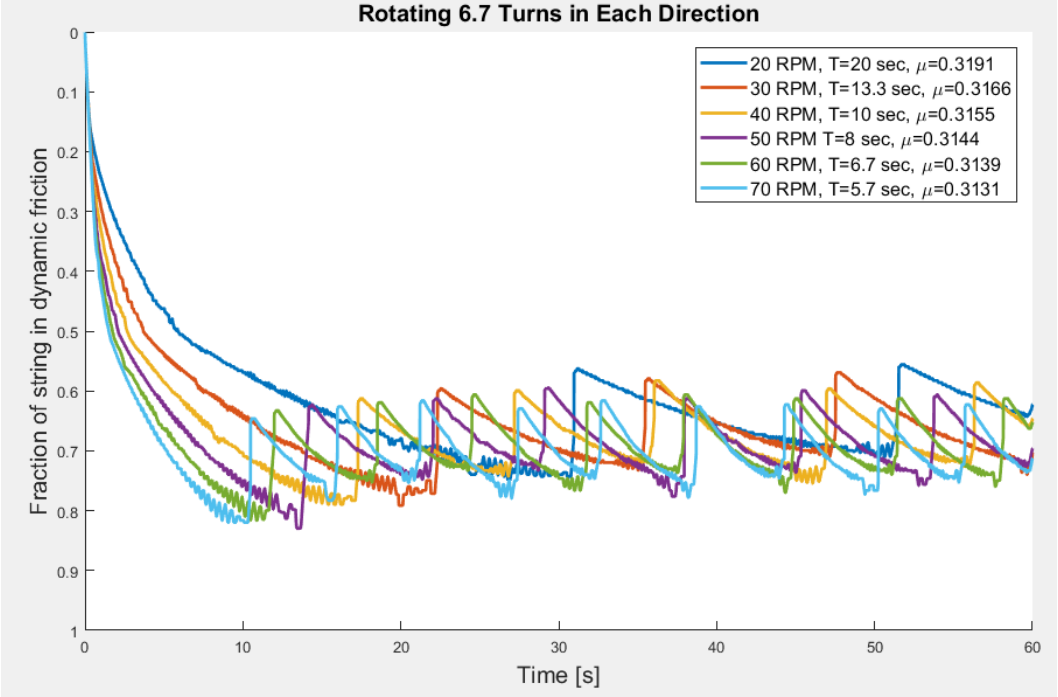


Figure 31: Regime variation keeping the number of turns in each direction constant.

The question now is how these cases should be evaluated to optimize the benefits of pipe rocking without losing control over toolface. The deeper the maximum rocking depth, the longer the section of the drillstring in dynamic motion, resulting in lower total

friction, allowing for better force transfer. However, the risk of transmitting the rotational energy all the way to the bit is increased in this case. Apart from that, if reactive torque produces significant vibrations, it would be easier to reach full rotation as it was shown in Figure 23. Maidla et al. (2004) showed that it is not possible to eliminate the pure sliding section of the drillstring (from the maximum rocking depth to the point of interference) without changing the toolface. A section of pure sliding is needed to provide good control of pipe movement.

The pipe rocking regime can be optimized by running several simulations and selecting the one that is found to be best for the operation. To quantify the effect of all the possible regimes, an equivalent overall FF is calculated. To do this, it is assumed that the maximum static FF is 25% higher than the dynamic FF. The equivalent FF is calculated as the weighted average per length of the static and dynamic FFs during a rocking operation, averaged in a one-minute window. Equation 42 shows an example calculation for the case when the maximum rocking depth is deeper than the cased section, with no reactive torque. In this equation, the dynamic FF of casing ($\mu_{casing}$) is multiplied by the length of the casing ($MD_{casing}$), the dynamic FF in the open hole, assumed to be $4/\pi$ times greater than $\mu_{casing}$ is multiplied by the section of the open hole with dynamic friction ($MD_{max\_roking}$-$MD_{casing}$), the static FF on the open hole, assumed to be 1.25 times the dynamic FF is multiplied by the length of the open hole under dynamic friction (*TD-MDmax_rocking*), and all this is divided by the total length of the well (*TD*). For the simulations shown in Figure 31, the overall FFs are, from the lowest RPM to the highest: 0.3191, 0.3166, 0.3155, 0.3144, 0.3139 and 0.3131. As it was expected, a higher RPM yields a smaller equivalent FF.

$$\mu_{avg} = \mu_{casing} \frac{MD_{casing} + \frac{4}{\pi}\left(MD_{\max\_rocking} - MD_{casing}\right) + 1.25\frac{4}{\pi}\left(TD - MD_{\max\_rocking}\right)}{TD} \quad \textbf{(42)}$$

Several simulations were run without considering reactive torque, as well as considering a maximum reactive torque of 2,000 lb-ft, with an RTC of 100ft/100lb-ft. This implies, the point of interference is 2,000 ft above the bit. The results of the simulations can be seen in Table 4. The grey cells are non-viable rocking regimes in which full rotation was reached. A color scale is used in which the red cells are the worst rocking regimes and the green ones are those with the smallest equivalent FF. The values bolded are those in between the smallest and largest FFs of the simulations shown in Figure 31. As can be seen in this figure, there are quite a few different combinations of RPM and time period that can yield similar results when it comes to pipe rocking.

| No Reactive Torque | | | | | | | | | |
|---|---|---|---|---|---|---|---|---|---|
| | | RPM | | | | | | | |
| | | 10 | 20 | 30 | 40 | 50 | 60 | 70 | 80 |
| Period [seconds] | 1 | 0.351 | 0.347 | 0.344 | 0.341 | 0.339 | 0.336 | 0.334 | 0.332 |
| | 2 | 0.349 | 0.344 | 0.340 | 0.336 | 0.333 | 0.329 | 0.326 | 0.324 |
| | 3 | 0.347 | 0.341 | 0.335 | 0.331 | 0.326 | 0.324 | 0.322 | 0.320 |
| | 4 | 0.345 | 0.338 | 0.332 | 0.326 | 0.323 | 0.321 | **0.318** | **0.316** |
| | 5 | 0.344 | 0.336 | 0.328 | 0.324 | 0.321 | **0.318** | **0.315** | **0.313** |
| | 6 | 0.343 | 0.334 | 0.326 | 0.322 | **0.318** | **0.315** | **0.313** | 0.310 |
| | 7 | 0.342 | 0.332 | 0.324 | 0.320 | **0.316** | **0.313** | 0.310 | 0.307 |
| | 8 | 0.340 | 0.329 | 0.323 | **0.318** | **0.314** | 0.311 | 0.308 | |
| | 9 | 0.339 | 0.328 | 0.322 | **0.317** | **0.313** | 0.309 | | |
| | 10 | 0.338 | 0.327 | 0.321 | **0.315** | 0.311 | 0.307 | | |
| | 12 | 0.336 | 0.325 | **0.318** | **0.313** | 0.308 | | | |
| | 14 | 0.335 | 0.323 | **0.316** | 0.310 | | | | |
| | 16 | 0.334 | 0.322 | **0.314** | 0.308 | | | | |
| | 18 | 0.332 | 0.320 | **0.312** | | | | | |
| | 20 | 0.331 | **0.319** | 0.311 | | | | | |
| | 25 | 0.328 | **0.316** | | | | | | |
| | 30 | 0.327 | **0.314** | | | | | | |
| | 35 | 0.326 | **0.312** | | | | | | |
| | 40 | 0.325 | | | | | | | |
| Maximum theoretical friction factor | | | | | | | | | 0.361 |
| Minimum theoretical friction factor | | | | | | | | | 0.289 |

| With Reactive torque | | | | | | | | | |
|---|---|---|---|---|---|---|---|---|---|
| | | RPM | | | | | | | |
| | | 10 | 20 | 30 | 40 | 50 | 60 | 70 | 80 |
| Period [seconds] | 1 | 0.342 | 0.339 | 0.336 | 0.333 | 0.330 | 0.328 | 0.325 | 0.323 |
| | 2 | 0.340 | 0.335 | 0.331 | 0.327 | 0.324 | 0.320 | **0.318** | **0.316** |
| | 3 | 0.338 | 0.332 | 0.327 | 0.322 | **0.318** | **0.315** | **0.313** | **0.311** |
| | 4 | 0.337 | 0.330 | 0.324 | **0.318** | **0.315** | **0.312** | 0.310 | 0.307 |
| | 5 | 0.335 | 0.327 | 0.320 | **0.316** | **0.312** | **0.310** | 0.307 | 0.304 |
| | 6 | 0.334 | 0.325 | **0.318** | **0.313** | 0.310 | 0.307 | 0.304 | |
| | 7 | 0.333 | 0.323 | **0.316** | **0.312** | 0.308 | 0.305 | | |
| | 8 | 0.332 | 0.321 | **0.314** | 0.310 | 0.306 | | | |
| | 9 | 0.331 | **0.319** | **0.313** | 0.308 | | | | |
| | 10 | 0.330 | **0.318** | **0.312** | 0.307 | | | | |
| | 12 | 0.328 | **0.316** | 0.310 | 0.304 | | | | |
| | 14 | 0.326 | **0.315** | 0.308 | | | | | |
| | 16 | 0.325 | **0.313** | 0.306 | | | | | |
| | 18 | 0.324 | **0.312** | | | | | | |
| | 20 | 0.322 | 0.311 | | | | | | |
| | 25 | 0.320 | 0.308 | | | | | | |
| | 30 | **0.319** | | | | | | | |
| | 35 | **0.318** | | | | | | | |
| | 40 | **0.316** | | | | | | | |
| Maximum theoretical friction factor | | | | | | | | | 0.352 |
| Minimum theoretical friction factor | | | | | | | | | 0.289 |

Table 4: Overall FFs for different simulations with and without reactive torque.

Table 4 indicates that it is preferable to choose regimes with lower RPM and longer time periods. This combination offers the following benefits: rotating slower allows for better control over the number of turns of the drillstring, making it easier to count them. If the driller decides to use time as the measure for his pipe rocking activity, the error in changing direction is lower with longer periods. Additionally, because the change in rotation from one direction to the other is abrupt, a lower RPM is less damaging for the surface and downhole equipment, particularly the drillstring itself. Specifically, the risk of having a back-off is reduced at a lower RPM. A higher RPM increases the angular momentum of the drillstring and can break a connection when backwards rotation occurs suddenly.

### 4.4 Effect of Pipe Rocking Regime on ROP

Figure 32 shows rocking operations for two wells drilled in the same area, with similar BHAs and well path, at approximately the same depth (red line). For simulation purposes, it is considered that both operations are done at 18,500 ft. It is assumed that the small changes in toolface (green line) are a consequence of noise in the measuring tools and not real changes in direction. Well #1 is rocked with 58 seconds intervals at 15 RPM, while Well #2 has a regime of 30 seconds per side, at 35 RPM. The average ROP (blue line) is 14.7 ft/hr for Well #1 and 22.2 ft/hr for Well #2, i.e. 51% higher than Well #1.

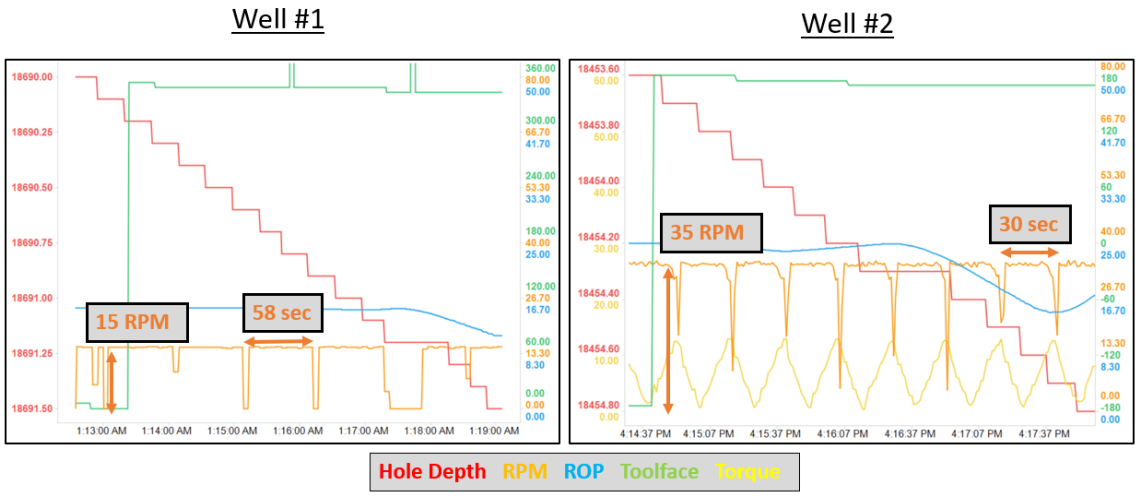


Figure 32: Field data for two similar wells being rocked at approximately the same depth.

Simulating these two cases shows that the well that is rocked at a higher RPM reaches a higher maximum rocking depth of around 13,875 ft, versus 12,580 ft for the other well (cf. Figure 33). Additionally, Well #2 transitions faster from the lowest to the maximum rocking depth. The overall FFs for these are 0.319 for Well #1 and 0.311 for Well #2. This difference in the FF is possibly one reason for the higher ROP in Well #2 (Figure 32).

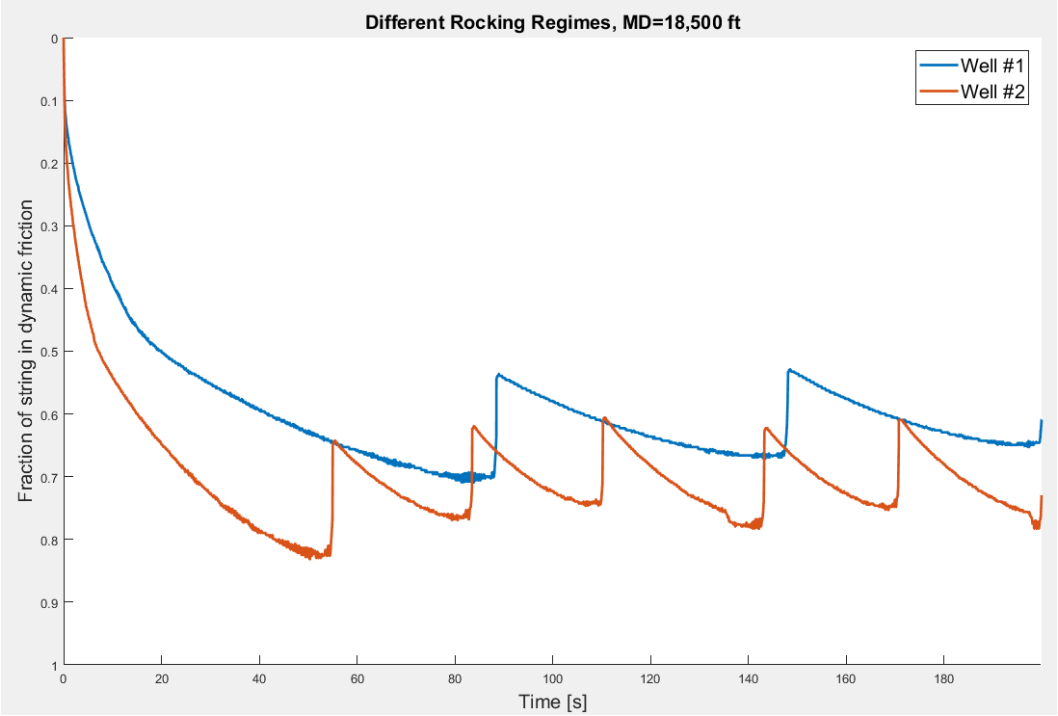


Figure 33: Simulation results for the two wells with similar rocking regime.

### 4.5 Pipe Rocking and Back-offs

Figure 34 shows the EDR data of a well that backed-off after a rocking operation at 18,300 ft. From 7:43 AM to 8:43 AM the string was oscillated at 65 RPM in 11-second periods. The crew noticed a decrease in 500 psi in standpipe pressure, and later realize that 11,500 ft of drill pipe had been disconnected from the rest of the string. Before the back-off, this BHA had drilled 190 ft in 19 hours, during which another section was slide drilled for 40 minutes, with a similar regime.

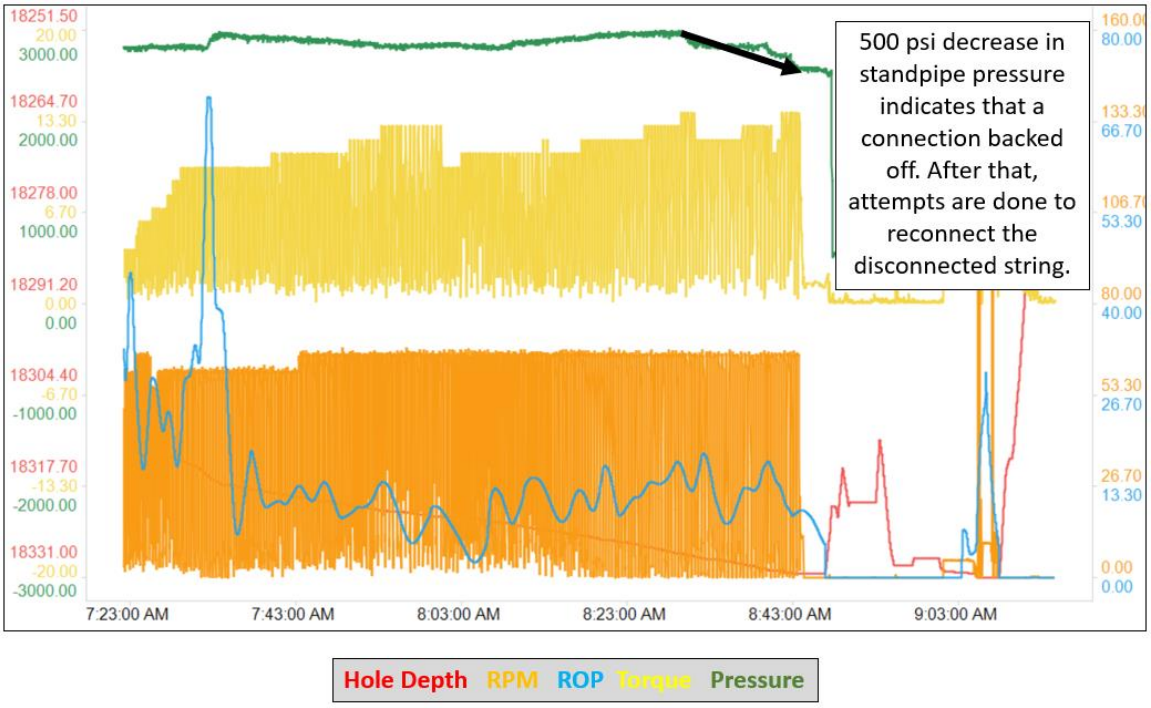


Figure 34: Example of how an aggressive rocking operation can potentially lead to a back-off.

In general, rocking at higher RPMs can potentially lead to back-offs, as higher angular momentum in the drilling tools can cause a joint to disconnect especially when suddenly changing the direction of rotation. To minimize the risk of having a back-off, it is recommended to use a rocking regime that achieves a similar effect at lower RPM. Figure 35 shows the results of rocking with the original regime versus another regime at 30 RPM with 24-second intervals. The maximum rocking depth is similar for these two cases, and the equivalent FFs are 0.3135 for the original case, and 0.3176 for the recommended one. The new regime expects to yield similar operational benefits, with a lower risk of backing-off a connection.

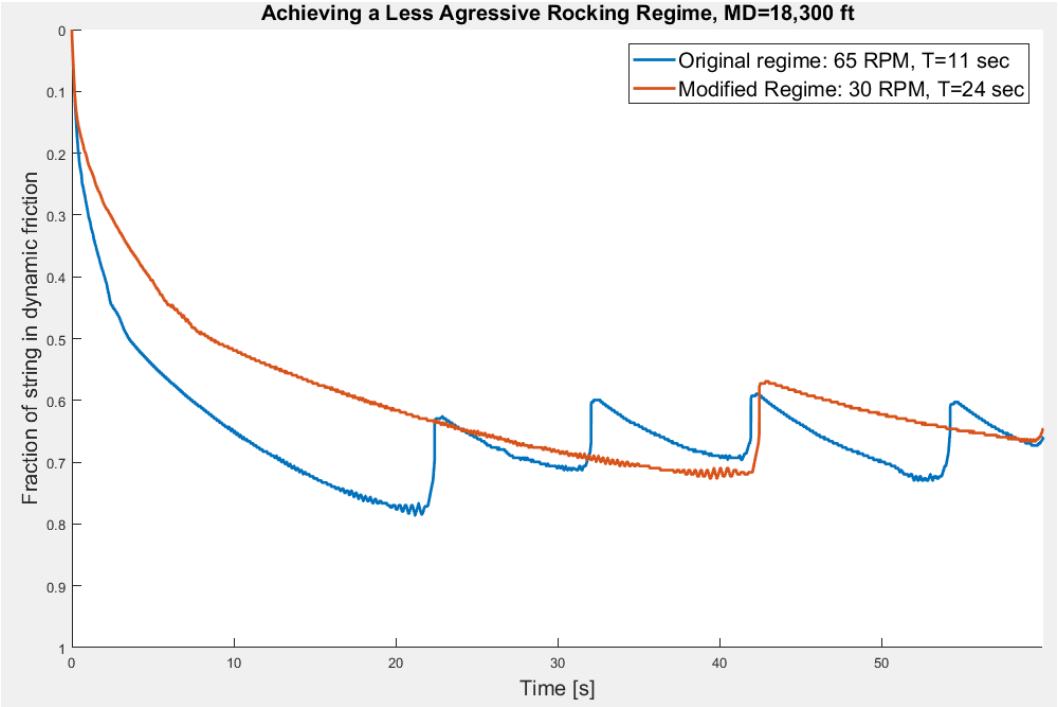


Figure 35: A less aggressive regime with longer intervals of rotation in each direction can bring similar operational benefits.

Also, when the string is rocked in a drilling operation, special attention should be given to the make-up torque of the connections. All the connections in the drillstring are designed to rotate to the right and disconnect to the left. For this reason, the risk of back-offs increases when rocking in the backwards direction. All the joints have a designed make-up and break-out torque that should never be exceeded during the operation. Often, the torque reported by the tools used for making the making the connections (top drive or iron roughneck) are not properly calibrated, giving misleading information on the value of the real make-up torque (Zenero et al., 2016).

Figure 36 shows a study done by Zenero et al. in 2016, where they used a separate calibrated sensor to measure the make-up torque and compared it to what an iron roughneck was reporting. They discovered that in many cases the iron roughneck was reporting

torques much higher than the real value. In some of these cases, the real make-up torque fell below typical operating values, compromising the connections specially during a rocking operation. For this reason, iron roughnecks should be calibrated periodically to guarantee they are making up the connections at the appropriate make up torque. Given this is still not widely done in the industry, it is best to use a simulator such as described in this chapter to identify low RPM regimes that satisfactorily reduce the overall friction during slide drilling operations.

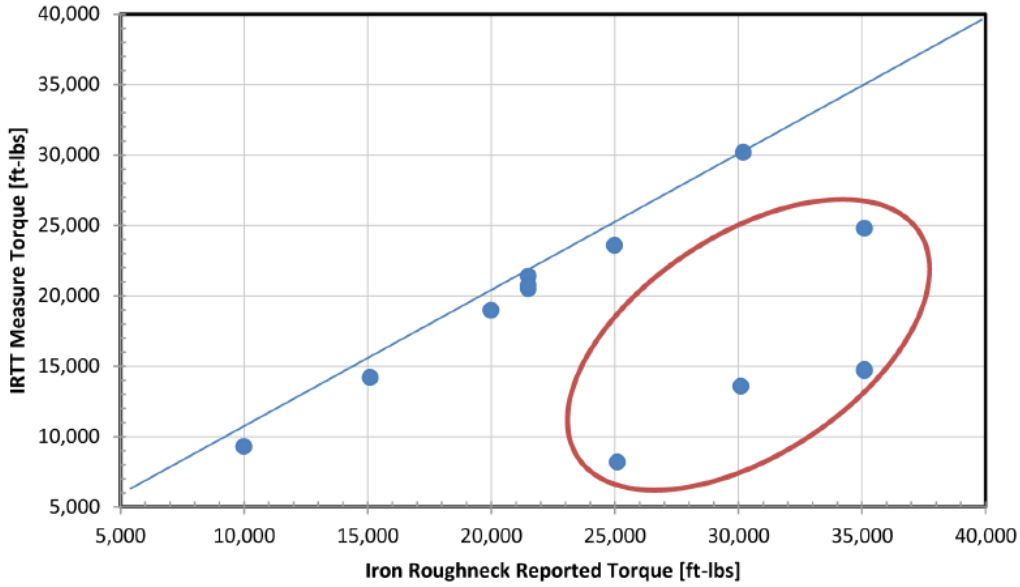


Figure 36: The iron roughneck reports torque much higher than the real torque. (Zenero et al., 2016)

# Chapter 5: Conclusions, Recommendations and Future Work

Continuous development of drilling technologies makes it now possible to unlock reserves which were technically or economically unrecoverable in the past. However, there is still a need to reduce drilling operation costs and increase wellbore quality to meet the changing markets worldwide. This thesis analyzed friction mitigation, which is one aspect of any drilling operation that can help improve wellbore quality and reduce costs when properly addressed.

## 5.1 CONCLUSIONS

The friction in a wellbore is generally quantified using the concept of torque (the surface torque required to rotate the string) and drag (the hook load when tripping or drilling the hole at different depths). These are dependent on the forces exerted by the segments of the drillstring against the hole, and the type of interface between the downhole tools and the open or cased hole.

Although friction is relevant to all types of drilling activity, this thesis was mainly focused on friction reduction practices when directional drilling with a downhole motor. One of the characteristics of slide drilling operations using downhole motors is that most of the drillstring (except the bit) remains static, resulting in high friction between the drillstring and the wellbore. This results in several problems including ROP, poor wellbore quality, and premature failure of downhole tools.

The model used in this thesis assumes that friction against the wellbore is a function of the normal force of the segments in the drillstring and the type of interaction between these segments and the wall. Friction mitigation practices are generally divided into three categories:

- Efforts to reduce the static FF.

- Efforts to reduce the normal force.
- Efforts to create a dynamic regime on sections of the well during slide drilling operations.

One way to reduce the static FF is by choosing an appropriate different drilling fluid. Though this, friction can often be reduced by more than 50%. In addition, many chemical and mechanical additives can be added to any type of mud to help further reduce friction. Generally, OBM and SOBM provide have better lubricating properties, but there are some reported cases in which HPWBM have outperformed these two. In addition, roller subs can be added to the drillstring to provide a rolling interface. To guarantee FFs, hole cleaning practices must be carried out thoroughly, as bed of cuttings on high angle and horizontal sections can easily block the small clearance between the pipes and the wellbore, severely increasing friction.

Normal forces can be managed through proper tool size selection. Lighter and shorter pipes with large ID is a good selection for these unconventional directional wells. In addition to the type of tools, the shape of the well also plays an important role in normal forces, as wells with higher DLS force the pipes to bend in a way that can increase tensions on the side and the contact area against the hole. Catenary curves, curvature-decreasing curves and circular arcs were found to be shapes that minimize friction.

Kinetic motion to break static friction can be achieved both by downhole tools or surface operations. Drilling agitator tools are used in a lot of unconventional drilling operation as they create an axial oscillation in the drillstring. It was found preferable to place the DAT 2,000 ft or more above the bit. Pipe rocking is an operation technique aimed at breaking static friction and consists of rotating the pipe forwards and backwards in an oscillatory fashion. This produces a rotational wave that travels through the drillstring breaking static friction in a limited section of the drillstring.

One of the main objectives of this work was to analyze and optimize pipe rocking operations. Typically, the rocking regimes for a sliding section are selected based on experience. Commercial technology that controls pipe rocking require manual input by the driller with regards to the RPM setpoint and number of wraps or periods of rotation to each side. Oilfield literature currently lacks a theoretical study of pipe rocking as well as simulators and analysis tools to help optimize pipe rocking. A simulator was therefore built as part of the work reported here, modeling the pipe rocking operation with a combination of a torque and drag model and the torsional damped wave equation. The main findings of the preliminary simulations are:

- Rotation on surface breaks static friction in a section of the well, giving better force transfer to the bit. These oscillations reach only a section of the well, up to the maximum rocking depth.
- The deeper the maximum rocking depth, the lower the friction and the better the weight and torque transfer to the bit. If the number of rotations is too high, the dynamic regime extends all the way to the bit and the rocking regime is termed "non-viable", and a reorienting process is then required.
- Reactive torque can produce vibrations in the lowest section of the drillstring. If the rotational wave from the pipe rocking reaches this zone of influence, the entire string rotates prematurely. If this is the case, it is found preferable to first address the vibrations and then optimize the rocking regime.
- Simulations showed that increasing the RPM or the number of rotations to each side increases the maximum rocking depth. They also showed that other rocking regimes that generate the same number of rotations to each side can yield similar results without the negatives of rotating at high RPM (see below).

- An equivalent friction factor can be used to quantify the effectiveness of the rocking regime. During a pipe rocking optimization exercise, several simulations can be run at different RPMs and periods of time to find those regimes that yield equivalent low friction factor values. This can also be done considering vibrations due to reactive torque. A lower equivalent friction factor allows for a better rocking operation.
- When possible, it is preferable to use rocking regimes with lower RPM and longer periods. This makes it easier for the driller to control the regime. Also, the reversals in direction are less harmful for surface and downhole tools when lower RPM is used. In particular, the risk of a connection back-off event is decreased.

### 5.2 RECOMMENDATIONS ON SIMULATOR USAGES

This section discusses recommendations in using the simulator. The simulator must first be calibrated properly. It is recommended that simulations be performed on several similar wells to obtain the damping coefficients that best work for these operations. Although downhole tools can provide more accurate calibrations, this could be systematically done with surface torque measurements which are always available. This process should yield a range of constants that represent the real operation quite accurately.

Then, the simulator should be used to come up with some rocking regimes that yield different maximum rocking depth. These should be tested to validate that cases in which deeper rocking depths result in higher ROPs and easier control over toolface. Also, rocking regimes should be selected for different drilling depths. It is recommended to find a combination of RPM and number of turns for every 500 ft to 1000 ft. The result should be a list of rocking regimes as a function of depth that the driller can use to have an idea of what rocking regime he or she should use for a sliding segment.

Finally, it must be noted that most of the friction reduction practices analyzed in this work are meant exclusively for directional drilling practices. A successful drilling job ultimately requires trouble-free casing run all the way to TD. It is recommended that a torque and drags analysis is performed before a casing running operations to ensure that the job can be completed.

## 5.3 FUTURE WORK

This thesis introduced the first pipe rocking simulator to better understand the physics of a pipe rocking operation and makes recommendations on rocking regimes to maximize its beneficial effects during sliding intervals.

The simulator was programed in Matlab and the next step is building an easy-to-use GUI. This GUI must be simple and comprehensive enough for field personnel to use without trouble. Also, it should be able to communicate with the other systems on the rig to obtain the contextual data needed (such as depth drilled, surveys, drill pipes, BHA, and mud density). Later, the program needs to go through field trials to improve its accuracy, helpfulness and field acceptance.

Additionally, the models used can be improved to better represent the physics of the problem. A stiff string torque and drag model can yield more accurate values of the normal force at each drillstring segment, which will then impact the damping coefficient used in the torsional damped wave equation. Finally, a drillstring model of downhole vibrations can be used to model the effect of reactive torque on the zone of influence's length. This can yield a more accurate estimation of the effect of reactive torque from the bit and its effects are on premature full rotation.

# Glossary

| Abbreviation | Meaning |
|---|---|
| BHA | Bottom Hole Assembly |
| DAS | Drilling Agitator System |
| DAT | Drilling Agitator Tool |
| DD | Directional Driller |
| DP | Differential Pressure |
| EDR | Electronic Drilling Recorder |
| ERD | Extended Reach Drilling |
| ERDW | Extended Reach Deviated Well |
| ERW | Extended Reach Well |
| FF | Friction Factor |
| HPWBM | High Performance Water Based Mud |
| MCM | Minimum Curvature Method |
| MWD | Measure While Drilling |
| NAF | Non-Aqueous Fluid |
| OBM | Oil Based Mud |
| RPM | Revolutions Per Minute |
| RSS | Rotary Steerable System |
| SOBM | Synthetic Oil Based Mud |
| SWOBT | Steady Weight on Bit Tool |
| TD | Total Depth |
| WBM | Water Based Mud |
| WOB | Weight on Bit |

# Symbols

| Symbol | Meaning |
|---|---|
| $\alpha$ | Azimuth |
| $c$ | Damping coefficient |
| $C$ | Damping Factor |
| $Ft$ | Tension force |
| $F_n$ | Normal force |
| $\mu$ | Friction factor |
| $\gamma$ | Shear strain |
| $G$ | Shear modulus |
| $J$ | Poplar moment of inertia |
| $RPM$ | RPM setpoint for rocking |
| $RPMmin$ | Minimum RPM for breaking static friction |
| $\tau$ | Shear stress |
| $\theta$ | Inclination |
| $t$ | Time |
| $T$ | Time rocking in each direction |
| $Tq_{reactive}$ | Maximum reactive torque |
| $Ø$ | Angular displacement |
| $Ømax$ | Maximum angular displacement for calculating $C$ |
| $w$ | Unit weight |
| $W$ | Weight |
| $z$ | Position / Measured depth |

# References


Aarrestad, T. V. (1994, September 1). Torque and Drag-Two Factors in Extended-Reach Drilling. Society of Petroleum Engineers. doi:10.2118/27491-PA

Aguilera, R., Cordell, G. M., Nicholl, G. W., Artindale, J.S., Ng, M.C. (1991, November 1). *Horizontal Wells: Formation Evaluation, Drilling, and Production, Including Heavy Oil Recovery.* Houston: Gulf Pub Co.

Alali, A., & Barton, S. P. (2011, January 1). Unique Axial Oscillation Tool Enhances Performance of Directional Tools in Extended Reach Applications. Society of Petroleum Engineers. doi:10.2118/143216-MS

Alfsen, T. E., Heggen, S., Blikra, H., & Tjotta, H. (1995, June 1). Pushing the Limits for Extended Reach Drilling: New World Record From Platform Statfjord C, Well C2. Society of Petroleum Engineers. doi:10.2118/26350-PA

Alley, S. D., & Sutherland, G. B. (1991, January 1). The Use of Real-Time Downhole Shock Measurements To Improve BHA Component Reliability. Society of Petroleum Engineers. doi:10.2118/22537-MS

Alshubbar, G. D., Coryell, T. N., Atashnezhad, A., Akhtarmanesh, S., & Hareland, G. (2017, August 28). The Effect of Barite Nanoparticles on the Friction Coefficient and Rheology of Water Based Mud. American Rock Mechanics Association.

Aslaksen, H., Annand, M., Duncan, R., Fjaere, A., Paez, L., & Tran, U. (2006, January 1). Integrated FEA Modeling Offers System Approach to Drillstring Optimization. Society of Petroleum Engineers. doi:10.2118/99018-MS

Barton, S. P., Baez, F., & Alali, A. (2011, January 1). Drilling Performance Improvements in Gas Shale Plays using a Novel Drilling Agitator Device. Society of Petroleum Engineers. doi:10.2118/144416-MS Bizanti, M. S., & Alkafeef, S. F. (2003, January 1). A Simplified Hole Cleaning Solution to Deviated and Horizontal Wells. Society of Petroleum Engineers. doi:10.2118/81412-MS

Buker, M. (2001, January 1). Advancements in Rotary Steerable Technology. Petroleum Society of Canada. doi:10.2118/2001-040-EA

Burnett, T., Gee, R., Martinez, J., Carson, C., Canuel, L. (2013). New Technology Enables Rigs with Limited Pump Pressure Capacity to Utilize the Latest Friction Reduction Technology. *SPE Eastern Regional meeting.*

Brett, J. F., Beckett, A. D., Holt, C. A., & Smith, D. L. (1989, September 1). Uses and Limitations of Drillstring Tension and Torque Models for Monitoring Hole Conditions. Society of Petroleum Engineers. doi:10.2118/16664-PA

Christiansen, C. (1991, January 1). From Oil-Based Mud to Water-Based Mud. Society of Petroleum Engineers. doi:10.2118/23359-MS

Codling, J. (2017, October 9). The Effect of Survey Station Interval on Wellbore Position Accuracy. Society of Petroleum Engineers. doi:10.2118/187249-MS

Duplantis, S. (2016). Slide Drilling – Farther and Faster. *Oilfield Review 28, no. 2.*

Dykstra, M. W., Neubert, M., Hanson, J. M., & Meiners, M. J. (2001, January 1). Improving Drilling Performance by Applying Advanced Dynamics Models. Society of Petroleum Engineers. doi:10.2118/67697-MS

EIA. (2015). *Annual Energy Outlook 2015: With Projections to 2040*. Government Printing Office.

EIA. (2016). Trends in US oil and natural gas upstream costs. *US Energy Information Administration*.

Falodun, S., Kellas, M., & Ehrunmwunsee, K. (2005, January 1). Optimal Horizontal Wellbore Placement Using New Drilling Technology In the Niger Delta - Bonga Field Case Study. World Petroleum Congress.

Fitzpatrick, R. (2013). *General Solution of 1D Wave Equation*. Retrieved January 22nd, 2019 from http://farside.ph.utexas.edu/teaching/315/Waves/node58.html.

Friedheim, J., & Sartor, G. (2003, January 1). WBM With Triple-Inhibition Mechanism Demonstrates Near-OBM Performance In Deepwater Gulf Of Mexico. Offshore Mediterranean Conference.

Fontenot, J. E. (1973, January 1). Factors Influencing Drag, Torque and Cost of Directional Drilling Near a Salt Dome. Society of Petroleum Engineers. doi:10.2118/4642-MS

Gaynor, T. M., Chen, D. C.-K., Stuart, D., & Comeaux, B. (2001, January 1). Tortuosity versus Micro-Tortuosity - Why Little Things Mean a Lot. Society of Petroleum Engineers. doi:10.2118/67818-MS

Gaynor, T., Hamer, D., Chen, D. C.-K., & Stuart, D. (2002, January 1). Quantifying Tortuosities by Friction Factors in Torque and Drag Model. Society of Petroleum Engineers. doi:10.2118/77617-MS

Gillan, C., Boone, S., Kostiuk, G., Schlembach, C., Pinto, J., & LeBlanc, M. G. (2009, January 1). Applying Precision Drill Pipe Rotation and Oscillation to Slide Drilling Problems. Society of Petroleum Engineers. doi:10.2118/118656-MS

Guild, G.J., Seymour, D.A., Hill, T.H. and Munro, R. (1993). Designing Extended Reach Wells. *Offshore Technical Drilling Conference.*

Guild, G.J and Jeffrey, J.T. (1994). Drilling Extended-Reach/High-Angle Wells Through Overpressured Shale Formation in the Central Graben Basin, Abroath Field, Block 22/17, U.K. North Sea.

Guild, G. J., Wallace, I. M., & Wassenborg, M. J. (1995, January 1). Hole Cleaning Program for Extended Reach Wells. Society of Petroleum Engineers. doi:10.2118/29381-MS

Haddad, M., AL-Aleeli, A. R., Zaheer, B., Ruzhnikov, A., Husien, M., & Marinescu, P. (2017, November 13). Drilling of Challenging ERD Wells with Water-Based Mud: How to Significantly Reduce Torque and Drag by New Generation Lubricant. Society of Petroleum Engineers. doi:10.2118/188796-MS

Hill, T. H., Guild, G. J., & Summers, M. A. (1996, June 1). Designing and Qualifying Drillstrings for Extended Reach Drilling. Society of Petroleum Engineers. doi:10.2118/29349-PA

Johancsik, C. A., Friesen, D. B., & Dawson, R. (1984, June 1). Torque and Drag in Directional Wells-Prediction and Measurement. Society of Petroleum Engineers. doi:10.2118/11380-PA

Jones, S., Feddema, C., Sugiura, J., & Lightey, J. (2016a, March 1). A New Friction Reduction Tool with Axial Oscillation Increases Drilling Performance: Field-Testing with Multiple Vibration Sensors in One Drillstring. Society of Petroleum Engineers. doi:10.2118/178792-MS

Jones, S., Feddema, C., & Sugiura, J. (2016b, March 1). A New Steady Weight-on-Bit Tool Reduces Torque and RPM Variations and Enhances Drilling Efficiency and Bit/BHA Life. Society of Petroleum Engineers. doi:10.2118/178818-MS

Kaarstad, E., Aadnoy, B. S., & Fjelde, T. (2009, January 1). A Study of Temperature Dependent Friction in Wellbore Fluids. Society of Petroleum Engineers. doi:10.2118/119768-MS

Kimball, C. F., Colwell, C. N., & Knell, J. W. (1991, January 1). A 78° Extended Reach Well in the Gulf of Mexico, Eugene Island 326 No. A-6. Offshore Technology Conference. doi:10.4043/6711-MS

Kercheville, J. D., Hinds, A. A., & Clements, W. R. (1986, January 1). Comparison of Environmentally Acceptable Materials With Diesel Oil for Drilling Mud Lubricity and Spotting Fluid Formulations. Society of Petroleum Engineers. doi:10.2118/14797-MS

Lafuente, M., & Granger, S. (2017, May 17). New Drill Pipe Size Improved Drilling Efficiency in Shale Plays. Society of Petroleum Engineers. doi:10.2118/185600-MS

Larsen, T. I., Pilehvari, A. A., & Azar, J. J. (1997, June 1). Development of a New Cuttings-Transport Model for High-Angle Wellbores Including Horizontal Wells. Society of Petroleum Engineers. doi:10.2118/25872-PA

Lowdon, R., Brands, S., & Alexander, G. (2015, March 17). Analysis of the Impact of Wellbore Tortuosity on Well Construction Using Scaled Tortuosity Index and High-Resolution Continuous Surveys. Society of Petroleum Engineers. doi:10.2118/173110-MS

Ma, S., Huang, G., Zhang, J., & Han, Z. (1998, January 1). Study on Design of Extended Reach Well Trajectory. Society of Petroleum Engineers. doi:10.2118/50900-MS

Maidla, E. E., & Wojtanowicz, A. K. (1990, September 1). Laboratory Study of Borehole Friction Factor With a Dynamic-Filtration Apparatus. Society of Petroleum Engineers. doi:10.2118/18558-PA.

Maidla, E., & Haci, M. (2004, January 1). Understanding Torque: The Key to Slide-Drilling Directional Wells. Society of Petroleum Engineers. doi:10.2118/87162-

Maidla, E. E., Haci, M., & Wright, D. (2009, January 1). Case History Summary: Horizontal Drilling Performance Improvement Due to Torque Rocking on 800 Horizontal Land Wells Drilled for Unconventional Gas Resources. Society of Petroleum Engineers. doi:10.2118/123161-MSMS

Mason, C. J., Williams, L. G., & Murray, G. N. (2000, January 1). Reinventing the Wheel - Reducing Friction in High-Angle Wells. Society of Petroleum Engineers. doi:10.2118/63270-MS

Mason, C. J., & Chen, D. C.-K. (2005, January 1). The Perfect Wellbore! Society of Petroleum Engineers. doi:10.2118/95279-MS.

Malcore, E. (2012). Reservoir drives choice of RSS vs mud motors. Drilling contractor, 68(2).

Malekzadeh, N., & Mohammadsalehi, M. (2011, January 1). Hole Cleaning Optimization in Horizontal Wells: A New Method To Compensate Negative Hole Inclination Effects. Society of Petroleum Engineers. doi:10.2118/143676-MS

McCormick, J. E., Evans, C. D., & Kirkpatrick, C. (2011, January 1). Ten Year Evolution and Field History of Design Changes for a Torque and Drag Reduction Performance Drilling Sub. Society of Petroleum Engineers. doi:10.2118/145987-MS

Menand, S. (2013, February). Borehole Tortuosity Effect on Maximum Horizontal Drilling Length Based on Advanced Buckling Modeling. In *Oral presentation of paper AADE-13-FTCE-21 at the AADE National Technical Conference and Exhibition, Oklahoma City, Oklahoma* (pp. 26-27).

Mitchell, R. F., & Samuel, G. R. (2007, January 1). How Good is the Torque-Drag Model? Society of Petroleum Engineers. doi:10.2118/105068-MS

Mitchell, R., & Miska, S. (2011). *Fundamentals of drilling engineering*. Society of Petroleum Engineers.

Mueller, M. D., Quintana, J. M., & Bunyak, M. J. (1990, January 1). Extended-Reach Drilling From Platform Irene. Society of Petroleum Engineers. doi:10.2118/20094-MS

Naganawa, S., Kudo, H., & Matsubuchi, H. (2017, December 1). Simulation Study on Influences of Wellbore Tortuosity on Hole Cleaning in Extended-Reach Drilling. Society of Petroleum Engineers. doi:10.2118/183409-PA

NOV (2016). *Agitator$^{TM}$ Systems Handbook.*

Rasheed, W. (2001, January 1). Extending the Reach and Capability of Non Rotating BHAs by Reducing Axial Friction. Society of Petroleum Engineers. doi:10.2118/68505-MS

Ravi, K., & Hemphill, T. (2006, January 1). Pipe Rotation and Hole Cleaning in Eccentric Annulus. Society of Petroleum Engineers. doi:10.2118/99150-MS

Samuel, R. (2010, January 1). Friction Factors: What are They for Torque, Drag, Vibration, Drill Ahead and Transient Surge/Swab Analysis. Society of Petroleum Engineers. doi:10.2118/128059-MS

Schamp, J. H., Estes, B. L., & Keller, S. R. (2006, January 1). Torque Reduction Techniques in ERD Wells. Society of Petroleum Engineers. doi:10.2118/98969-MS

Schaaf, S., Mallary, C. R., & Pafitis, D. (2000, January 1). Point-the-Bit Rotary Steerable System: Theory and Field Results. Society of Petroleum Engineers. doi:10.2118/63247-MS

Shor, R. J. (2016, May). The effect of well path, tortuosity and drillstring design on the transmission of axial and torsional vibrations from the bit and mitigation control strategies (Doctoral dissertation).

Skyles, L., Amiraslani, Y., & Wilhoit, J. (2012, January 1). Converting Static Friction to Kinetic Friction to Drill Further and Faster in Directional Holes. Society of Petroleum Engineers. doi:10.2118/151221-MS

Sugiura, J., & Jones, S. (2010, January 1). Rotary Steerable System Enhances Drilling Performance on Horizontal Shale Wells. Society of Petroleum Engineers. doi:10.2118/131357-MS

Tanguy, D. R., & Zoeller, W. A. (1981, January 1). Applications Of Measurements While Drilling. Society of Petroleum Engineers. doi:10.2118/10324-MS

Tomren, P. H., Iyoho, A. W., & Azar, J. J. (1986, February 1). Experimental Study of Cuttings Transport in Directional Wells. Society of Petroleum Engineers. doi:10.2118/12123-PA

Tveitan, K. (2011). *Torque and drag analyses of North Sea wells using new 3D model*. (Master's thesis, University of Stavanger, Norway).

Yadav, P., Kosandar, B. A., Jadhav, P. B., Ishaq, L. G., Addagalla, A. K. V., & Mohammad, A. R. (2015, March 8). Customized High-Performance, Water-Based

Mud for Unconventional Reservoir Drilling. Society of Petroleum Engineers. doi:10.2118/172603-MS

Yim, M., Healey, S., Leedham, R., Giuliano, M., Weber, M., & Pitre, D. (2015, October 20). Drillstring Torque Reducing Technology Improves Drilling Efficiency in Horizontal Well. Society of Petroleum Engineers. doi:10.2118/176134-MS

Warren, T. M. (2006, January 1). Steerable Motors Hold Their Own Against Rotary Steerable Systems. Society of Petroleum Engineers. doi:10.2118/104268-MS

Weijermans, P., Ruszka, J., Jamshidian, H., & Matheson, M. (2001, January 1). Drilling with Rotary Steerable System Reduces Wellbore Tortuosity. Society of Petroleum Engineers. doi:10.2118/67715-MS

Worford, S. W., & Craig, P. G. (1983, January 1). Shock Absorbers - Are They Necessary? Society of Petroleum Engineers. doi:10.2118/11406-MS

Zenero, N., Koneti, S., & Schnieder, W. (2016, March 1). Iron Roughneck Make Up Torque - Its Not What You Think! Society of Petroleum Engineers. doi:10.2118/178776-MS

Zhang, F., Filippov, A., Miska, S., & Yu, M. (2017, March 6). Hole Cleaning and ECD Management for Drilling Ultra-Long-Reach Laterals. Society of Petroleum Engineers. doi:10.2118/183786-MS